AIMS Mathematics, 11(10): 34583–34614.
DOI: 10.3934/math.20261348
Received: 24 August 2026
Revised: 06 October 2026
Accepted: 19 October 2026
Published: 23 October 2026

http://www.aimspress.com/journal/Math

Research article

Analysis of impulsive neutral Caputo fractional Volterra–Fredholm integro-differential systems with applications to Solana cryptocurrency modeling

Prabakaran Raghavendran[1], Yamini Parthiban[2], Shyam Sundar Santra[3] and Mohammadjavad Habibivostakolaei[4,*]

[1] Center for Research, Easwari Engineering College, 18 Bharathi Salai, Ramapuram, Chennai 600089, Tamil Nadu, India; Email: rockypraba55@gmail.com
[2] Department of Mathematics, SRM Institute of Science and Technology, Ramapuram, Chennai 600089, Tamil Nadu, India; Email: yaminiparthiban.msc@gmail.com
[3] Department of Mathematics, JIS College of Engineering, Kalyani, West Bengal 741235, India; Email: shyamsundar.santra@jiscollege.ac.in
[4] Institute of Mathematics, Henan Academy of Sciences, Zhengzhou 450046, China; Email: mjhabibi@hnas.ac.cn

* **Correspondence:** Email: mjhabibi@hnas.ac.cn; Tel: +86-13949108621.

Abstract: This study investigated an impulsive neutral Volterra–Fredholm integro-differential equation (VFIDE) involving the Caputo fractional derivative and developed a mathematical framework for establishing the existence and controllability of solutions. Under appropriate assumptions on the fractional order, nonlinear functions, and integral operators, the existence of solutions was established using the Schauder fixed-point theorem, while controllability was analyzed through an admissible control formulation. The proposed model incorporates fractional memory effects, Volterra–Fredholm nonlocal interactions, and abrupt state changes through impulsive terms. A fully specified numerical example was presented using a product-integration scheme, numerical quadrature, and fixed-point iteration, with grid refinement used to examine numerical stability. The framework was further illustrated using daily Solana cryptocurrency closing-price data from January 1 to December 1, 2025. The results demonstrate the applicability of the proposed framework to fractional impulsive dynamical modeling.

Keywords: fractional differential equations; impulsive systems; Volterra–Fredholm integro-differential equations; controllability; Solana cryptocurrency
Mathematics Subject Classification: 26A33, 34A08, 34K35, 45G10

1. Introduction

Fractional differential and integro-differential equations can be employed to describe memory processes, hereditary dependence and nonlocal interactions in the context of dynamical processes. They are well-developed in the literature both theoretically and in terms of their application; see, for example, [1, 2]. Ahmad and Sivasundaram [3] discussed the existence results for fractional integro-differential equations under nonlinear conditions and Harikrishnan et al. [4] examined the existence and stability of fractional integro-differential equations with a generalized proportional fractional derivative. To analyze fractional dynamical systems, another approach is to generalize the fractional derivative proposed by Hattaf with a non-singular kernel [5].

Volterra–Fredholm integro-differential equations are an important class of integro-differential equations that are integral dependent across a variable interval and fixed interval. Hamoud and Ghadle [6] considered uniqueness results for the fractional Volterra–Fredholm integro-differential equations, also Hamoud et al. [7] obtained the existence and uniqueness results for Volterra–Fredholm integro-differential equations. The existence and uniqueness of solutions to Volterra–Fredholm integro-differential equations with the Caputo fractional derivative was investigated by Ndiaye and Mansal [8]. From a numerical perspective, Toma and Postavaru [9] considered a fractional Fredholm–Volterra integro-differential equation of the form

$$h_1\left(x, f(x), D^{\alpha_1} f(x), D^{\alpha_2} f(x), \ldots, D^{\alpha_k} f(x)\right) = \lambda h_2\left(x, f(x), \int_0^x p(x,s) G(s, f(s))\, ds\right), \tag{1.1}$$

subject to the initial conditions

$$D^j f(0) = f_j, \qquad j = 1, 2, \ldots, k. \tag{1.2}$$

The solution was presented in the form of a formulation that incorporates fractional derivatives and Volterra-type integral dependence in the Fredholm–Volterra problem. Numerical algorithms for nonlinear Volterra–Fredholm integro-differential equations were also developed by HamaRashid et al. [10] and reproducing-kernel techniques for systems of Volterra integral equations were investigated by Jiang and Chen [11].

The mixture of fractional dynamics, fractional control, and fractional Volterra–Fredholm operators has also been the subject of attention. In Hussain et al.'s work [12], existence and controllability problems of fractional semilinear mixed Volterra–Fredholm integro-differential equations were investigated. Their model can be represented by

$$\begin{cases} {}^{C}D^{\gamma} u(q) = \mathcal{A}u(q) + \mathcal{B}x(q) + g\left(q, u(q), \displaystyle\int_0^q h(q, r, u(r))\, dr, \int_0^S k(q, r, u(r))\, dr\right), \\ \qquad u(0) = u_0 + \rho(u), \qquad u'(0) = u_1 + \varphi(u), \end{cases} \quad q \in J = [0, S]. \tag{1.3}$$

This system includes Volterra and Fredholm integral contributions, with a Caputo fractional derivative and a control operator. Therefore it offers a similar structure to the present problem, but not at the same time as the neutral functional and instantaneous impulsive structures that are studied here.

Controllability has been also studied in other types of fractional evolution systems. In Banach spaces, controllability of Volterra–Fredholm-type systems was studied by Hernández and O'Regan [13]

and fractional stochastic Volterra–Fredholm integro-differential systems of order $1 < r < 2$ were studied by Dineshkumar et al. [14]. Classical results on controllability and stability were given by Jurdjevic and Quinn [15]. Hussain et al. [16] considered mild solutions and controllability for fractional evolution inclusions of Clarke's subdifferential type. Their model is given by

$$\begin{cases} {}^{C}D_{\tau}^{q} r(\tau) \in \mathcal{A}r(\tau) + \mathcal{B}u(\tau) + E\partial Q(\tau, r(\tau)), & \tau \in U = [0, \sigma], \\ r(0) + m(r) = r_0, \qquad r'(0) + n(r) = r_1. \end{cases} \tag{1.4}$$

The inclusion structure and the nonlocal conditions in this model are different from the nonlinear neutral Volterra–Fredholm system studied in the present paper. Hussain et al. [17] also derived the controllability results of fractional differential evolution equations of order $\gamma \in (1, 2)$ under nonlocal conditions. Their formulation contains a Caputo fractional derivative, a control term, and a Volterra integral contribution, namely,

$$\begin{cases} {}^{C}D_{\tau}^{\gamma} r(\xi) = \mathcal{A}r(\xi) + \mathcal{B}v(\xi) + g(\xi, r(\xi)) + \displaystyle\int_0^{\xi} p(\xi - \zeta) f(\zeta, r(\zeta))\, d\zeta, \\ r(0) + n(r) = r_0, \qquad r'(0) + m(r) = r_1, \end{cases} \qquad \xi \in J = [0, K]. \tag{1.5}$$

The results show the importance of fractional operators, integral terms, and control functions in the controllability analysis.

The impulsive effects are also introduced as another representation of sudden changes in a dynamical system. Gautam et al. [18] studied the controllability of the abstract fractional differential equation with an impulsive effect. Gautam et al. [19] discussed impulsive fractional functional differential equations (IFFDEs) with a state-dependent delay and trajectory controllability in a related study. Their system is described by

$${}^{C}D_{\tau}^{r} h(\tau) = Ah(\tau) + f\left(\tau, h_{\rho(\tau, h_\tau)}\right), \qquad \tau \in J, \quad \tau \neq \tau_k, \tag{1.6}$$

together with the impulsive conditions

$$\Delta h(\tau_k) = I_k\left(h(\tau_k^-)\right), \qquad \Delta h'(\tau_k) = Q_k\left(h(\tau_k^-)\right), \qquad k = 1, 2, \ldots, m. \tag{1.7}$$

The results of these studies highlight the role of impulsive mechanisms in fractional controllability problems. The existence and controllability of fractional integro-differential inclusions with impulsive effects was further studied by Mohan Raja et al. in [20].

Other similar formulations use delay and Sobolev-type structures. In two recent papers, Ma et al. [21] examined approximate controllability of fractional delay integro-differential systems with a Sobolev-type operator. Their formulation includes a Caputo fractional derivative, a Volterra integral term, infinite delay, a multivalued nonlinear component, and a control operator:

$$\begin{cases} {}^{C}D_{\zeta}^{r}[Nz(\zeta)] \in Az(\zeta) + \mathbb{E}(\zeta, z_\zeta) + \displaystyle\int_0^{\zeta} h(\zeta, \beta, z_\beta)\, d\beta + \mathbb{B}x(\zeta), \\ z(0) = \varphi(0) + \mu(z_{\zeta_1}, z_{\zeta_2}, \ldots, z_{\zeta_k}), \qquad z'(0) = z_1. \end{cases} \tag{1.8}$$

This formulation differs from the present system by the Sobolev-type operator, infinite-delay structure, and multivalued nonlinearity.

In other application areas, the role of fractional operators in models with control was also studied. Johnson et al. [22] discussed the optimal control of fractional differential hemivariational inequalities, and Sadek [23] dealt with control theory on fractional differential Sylvester matrix equations with a Caputo derivative. A model for fractional optimal control of endometrial cancer treatment based on Caputo fractional derivatives was developed by Ramalakshmi and Samei [24]. The studies highlight the wide range of applicability of fractional operators in mathematical control problems.

Aljarallah et al. [25] considered Caputo–Fabrizio fractional integro-differential equations with non-instantaneous impulsive effects more recently. Their principal problem is formulated as

$$\begin{cases} {}^{CF}D^{\delta}z(\vartheta) = F(\vartheta, z(\vartheta), Bz(\vartheta)), & \vartheta \in (\kappa_i, \vartheta_{i+1}], \\ z(\vartheta) = H_i(\vartheta, z(\vartheta)), & \vartheta \in (\vartheta_i, \kappa_i], \\ z(b) - z'(b) = \displaystyle\int_b^T G(\kappa, z(\kappa))\, d\kappa, \end{cases} \tag{1.9}$$

where the integral operator is defined by

$$Bz(\vartheta) = \int_0^{\vartheta} x(\vartheta, \kappa, z(\kappa))\, d\kappa. \tag{1.10}$$

This work is relevant as it deals with the combination of fractional integro-differential dynamics, integral dependence, and impulsive effects, but with the Caputo–Fabrizio derivative and non-instantaneous impulses. Recently, Sher et al. [26] studied coupled systems of fractional integro-differential equations with the help of the conformable fractional derivative, where they applied analytical and computational methods to continue the development of fractional integro-differential modeling with modern numerical and learning methods.

Integro-differential equations have also been applied to financial mathematical models. Antipov and Kabanov [27] derived an integro-differential equation for the survival probability in a non-life insurance model with investment, given by

$$\frac{1}{2}\kappa^2\sigma^2u^2G''(u) + ((a-r)\kappa + r)uG'(u) + cG'(u) + \lambda \int_0^{\infty} [G(u-y) - G(u)]\, dF(y) = 0. \tag{1.11}$$

This study demonstrates the applicability of integro-differential equations to financial mathematical modeling and provides additional motivation for investigating nonlocal mathematical structures in financial applications.

Thus, the literature shows that fractional derivatives, Volterra–Fredholm operators, control inputs, neutral dependence, impulsive effects, delay structures, and nonlocal conditions have been studied in various related scenarios. In particular, analytical and numerical studies of fractional Volterra–Fredholm models were studied in [6–10] and, for Volterra–Fredholm systems and a couple of classes of fractional evolution equations, controllability was studied in [12–14, 16, 17]. Fractional controllability has also been studied in the case of impulsive fractional controllability in [18–20] and neutral Caputo fractional integro-differential systems were recently studied in [28]. But taking into account a neutral functional term along with the Caputo fractional differentiations, considering both the Volterra and Fredholm integral operators, as well as the instantaneous impulsive conditions and the controllability within a unified system, is a topic of future study.

Inspired by this research gap, the present study explores the impulsive neutral Caputo fractional Volterra–Fredholm integro-differential system considered in Section 3. The solution's existence is proven by the Schauder fixed point theorem [29] and the construction of the control operator and right inverse. The case study is a fully specified numerical example, in which the fractional component is approximated by product integration, the Volterra and Fredholm terms are approximated numerically, and the fixed point iteration is used. Grid-refinement calculations are also carried out to investigate the numerical stability of the implementation.

The proposed framework is further illustrated using daily Solana cryptocurrency closing-price data. The fractional component is used to represent memory characteristics, the Volterra and Fredholm terms incorporate nonlocal contributions, and the impulsive component represents abrupt variations identified from the observed price-change series. The controllability formulation is employed for controlled scenario analysis rather than being presented as a fully validated cryptocurrency forecasting model. The application therefore provides a real-data illustration of the proposed mathematical framework.

The remainder of this paper is organized as follows. Section 2 introduces the preliminary concepts and definitions required for the subsequent analysis. Section 3 presents the formulation of the impulsive neutral Caputo fractional Volterra–Fredholm integro-differential system and the assumptions used in the analysis. Section 4 establishes the main existence and controllability results. Section 5 presents the numerical example and describes the numerical procedure used for its implementation. Section 6 provides the graphical representation of the numerical results. Section 7 presents the application of the proposed framework to Solana cryptocurrency price modeling and controlled scenario analysis. Finally, Section 8 summarizes the main conclusions and discusses possible directions for future research.

2. Preliminaries

Here, we focus on the common definitions employed in fractional calculus, as previously discussed in academic literature [28]. Let $\mathcal{J} = [\varphi_0, b]$ with $\varphi_0 < \varphi_1 < \cdots < \varphi_m < \varphi_{m+1} = b$ denote the considered interval with prescribed impulsive points. We consider the piecewise continuous function space $PC(\mathcal{J}; \mathcal{X})$, consisting of all functions $\psi : \mathcal{J} \to \mathcal{X}$ that are continuous on each interval $(\varphi_k, \varphi_{k+1}]$ and possess finite left and right limits at every impulsive point φ_k, $k = 1, 2, \ldots, m$. The space $PC(\mathcal{J}; \mathcal{X})$ is endowed with the supremum norm

$$\|\psi\|_\infty = \sup_{\varphi \in \mathcal{J}} \|\psi(\varphi)\|_{\mathcal{X}}.$$

At each impulsive point φ_k, we adopt the right-continuous representative $\psi(\varphi_k) = \psi(\varphi_k^+)$, while $\psi(\varphi_k^-)$ and $\psi(\varphi_k^+)$ denote the corresponding left and right limits, respectively.

Definition 2.1. [2] For a function $\phi \in AC([\varphi_0, b]; \mathcal{X})$, the Caputo fractional derivative of order $\aleph$, where $0 < \aleph < 1$, is defined by

$${}^{C}D^{\aleph}_{\varphi_0+}\phi(\omega) = \frac{1}{\Gamma(1-\aleph)} \int_{\varphi_0}^{\omega} (\omega - s)^{-\aleph} \phi'(s)\, ds, \qquad \omega \in (\varphi_0, b].$$

For $\mathcal{X}$-valued functions, the integral is understood in the Bochner sense.

Theorem 2.1 (Arzelà–Ascoli theorem)**.** *Let $\mathcal{X}$ be a Banach space and let $\mathcal{F} \subset C([\varphi_0, b]; \mathcal{X})$. Then $\mathcal{F}$ is relatively compact in $C([\varphi_0, b]; \mathcal{X})$ if and only if $\mathcal{F}$ is equicontinuous and $\{\psi(\varphi) : \psi \in \mathcal{F}\}$ is relatively compact in $\mathcal{X}$ for every $\varphi \in [\varphi_0, b]$. For the impulsive setting, this criterion is applied separately on each interval $(\varphi_k, \varphi_{k+1}]$, together with the existence of the corresponding one-sided limits at the impulse points.*

Theorem 2.2. (Schauder fixed point theorem, see [4, 29]) Let $\mathcal{X}$ be a Banach space and B a nonempty subset of $\mathcal{X}$ that is both closed and convex. Suppose $N : B \to B$ is a continuous mapping and the image $N(B)$ is relatively compact in $\mathcal{X}$. Then, N has at least one fixed point in B.

3. Existence results

In this section, we explore the Caputo fractional impulsive VFIDE, given by:

$$\begin{aligned} {}^{C}D^{\aleph}\Big[\psi(\varphi) - \xi_1(\varphi, \psi(\varphi))\Big] &= \Upsilon(\varphi)\psi(\varphi) + \xi_2(\varphi, \psi(\varphi)) + \int_{\varphi_0}^{\varphi} \zeta_1(\varphi, \varpi, \psi(\varpi))d\varpi \\ &\quad + \int_{\varphi_0}^{b} \zeta_2(\varphi, \varpi, \psi(\varpi))d\varpi, \\ \Delta\psi(\varphi_k) &= \psi(\varphi_k^+) - \psi(\varphi_k^-) = I_k(\psi(\varphi_k^-)), \qquad k = 1, 2, \ldots, m. \end{aligned} \tag{3.1}$$

The initial condition that accompanies this equation is

$$\psi(\varphi_0) = \psi_0. \tag{3.2}$$

In the above expressions, ${}^{C}D^{\aleph}$ denotes the Caputo fractional derivative with $0 < \aleph \leq 1$, and $\psi \in PC(\mathcal{J}; \mathcal{X})$, where $\mathcal{J} = [\varphi_0, b]$, represents the piecewise continuous state function under consideration. Additionally, the functions $\xi_i : \mathcal{J} \times \mathcal{X} \to \mathcal{X}$ and $\zeta_i : \mathcal{J} \times \mathcal{J} \times \mathcal{X} \to \mathcal{X}$ are also continuous functions for $i = 1, 2$. Here $\Delta = \{(\varphi, \psi) : 0 \leq \varphi_0 \leq \psi \leq \varphi \leq b\}$, $0 < \varphi_0 < \varphi_1 < \varphi_2 < \cdots < \varphi_m < \varphi_{m+1} = b$, $\Delta\psi(\varphi_k) = \psi(\varphi_k^+) - \psi(\varphi_k^-)$, $\psi(\varphi_k^+)$, $\psi(\varphi_k^-)$ denote the right and left limits of ψ at φ_k, respectively.

Before examining our primary results and their proofs, we first introduce the following lemma along with several essential hypotheses:

($B1$) Let $\zeta_1 : D_V \times \mathcal{X} \to \mathcal{X}$ and $\zeta_2 : D_F \times \mathcal{X} \to \mathcal{X}$ be continuous functions, where $D_V = \{(\varphi, \varpi) \in \mathcal{J} \times \mathcal{J} : \varphi_0 \leq \varpi \leq \varphi \leq b\}$ is the Volterra triangular domain and $D_F = \mathcal{J} \times \mathcal{J}$ is the Fredholm domain. They satisfy the following conditions:

$$\begin{aligned} \|\zeta_1(\varphi, \varpi, \psi_1(\varpi)) - \zeta_1(\varphi, \varpi, \psi_2(\varpi))\| &\leq L_{\zeta_1}\|\psi_1(\varpi) - \psi_2(\varpi)\|, \\ \|\zeta_2(\varphi, \varpi, \psi_1(\varpi)) - \zeta_2(\varphi, \varpi, \psi_2(\varpi))\| &\leq L_{\zeta_2}\|\psi_1(\varpi) - \psi_2(\varpi)\|; \end{aligned}$$

($B2$) The functions ξ_1 and ξ_2, both defined as mappings from $\mathcal{J} \times \mathcal{X}$ to $\mathcal{X}$, are continuous and fulfill the conditions

$$\begin{aligned} \|\xi_1(\varphi, \psi_1) - \xi_1(\varphi, \psi_2)\| &\leq L_{\xi_1}\|\psi_1 - \psi_2\|, \\ \|\xi_2(\varphi, \psi_1) - \xi_2(\varphi, \psi_2)\| &\leq L_{\xi_2}\|\psi_1 - \psi_2\|; \end{aligned}$$

($B3$) The function $\Upsilon : \mathcal{J} \to \mathcal{L}(\mathcal{X})$ is continuous, where $\mathcal{L}(\mathcal{X})$ denotes the Banach space of bounded linear operators from $\mathcal{X}$ into itself. In addition, the constants L_{ζ_1}, L_{ζ_2}, L_{ξ_1}, and L_{ξ_2} are positive. We further define $\|\Upsilon\|_\infty = \sup_{\varphi \in \mathcal{J}} \|\Upsilon(\varphi)\|_{\mathcal{L}(\mathcal{X})} < \infty$.

($B4$) The constants $L_{\zeta_1}^*$, $L_{\zeta_2}^*$, $L_{\xi_1}^*$, and $L_{\xi_2}^*$ are defined by

$$L_{\zeta_1}^* = \sup_{(\varphi, \varpi) \in D_V} \|\zeta_1(\varphi, \varpi, 0)\|, \qquad L_{\zeta_2}^* = \sup_{(\varphi, \varpi) \in D_F} \|\zeta_2(\varphi, \varpi, 0)\|,$$

$$L^*_{\xi_1} = \sup_{\varphi\in\mathcal{J}} \|\xi_1(\varphi, 0)\|, \qquad L^*_{\xi_2} = \sup_{\varphi\in\mathcal{J}} \|\xi_2(\varphi, 0)\|;$$

($B5$) There exist constants $\lambda_1^* > 0$ and $\lambda_2^* > 0$ such that $\|I_k(\psi_1) - I_k(\psi_2)\| \le \lambda_1^* \|\psi_1 - \psi_2\|$ and $\|I_k(\psi)\| \le \lambda_2^*$ for all $\psi, \psi_1, \psi_2 \in \mathcal{X}$ and $k = 1, 2, \ldots, m$, where $I_k : \mathcal{X} \to \mathcal{X}$.
($B6$) For every $\gamma > 0$ and every $\varphi \in \mathcal{J}$, the set

$$\Big\{(\vartheta\psi)(\varphi) : \psi \in \Lambda_\gamma\Big\}$$

is relatively compact in $\mathcal{X}$. In particular, the set

$$\Big\{\xi_1(\varphi, \psi(\varphi)) : \psi \in \Lambda_\gamma\Big\}$$

is relatively compact in $\mathcal{X}$ for every $\varphi \in \mathcal{J}$.

Lemma 3.1. If $\psi_0(\varphi) \in PC(\mathcal{J}; \mathcal{X})$, then $\psi(\varphi) \in PC(\mathcal{J}; \mathcal{X})$ is a solution to problem (3.1)–(3.2) if and only if it satisfies the following integral equation:

$$\begin{aligned}
\psi(\varphi) = {} & \psi_0 - \xi_1(\varphi_0, \psi_0) + \xi_1(\varphi, \psi(\varphi)) + \frac{1}{\Gamma(\aleph)} \int_{\varphi_0}^{\varphi} (\varphi - \varpi)^{\aleph-1} \Upsilon(\varpi)\psi(\varpi)\, d\varpi \\
& + \frac{1}{\Gamma(\aleph)} \int_{\varphi_0}^{\varphi} (\varphi - \varpi)^{\aleph-1} \xi_2(\varpi, \psi(\varpi))\, d\varpi \\
& + \frac{1}{\Gamma(\aleph)} \int_{\varphi_0}^{\varphi} (\varphi - \varpi)^{\aleph-1} \int_{\varphi_0}^{\varpi} \zeta_1(\varpi, \omega, \psi(\omega))\, d\omega\, d\varpi \\
& + \frac{1}{\Gamma(\aleph)} \int_{\varphi_0}^{\varphi} (\varphi - \varpi)^{\aleph-1} \int_{\varphi_0}^{b} \zeta_2(\varpi, \omega, \psi(\omega))\, d\omega\, d\varpi \\
& + \sum_{\varphi_k < \varphi} I_k(\psi(\varphi_k^-))
\end{aligned} \tag{3.3}$$

for $\varphi \in (\varphi_k, \varphi_{k+1}]$, $k = 0, 1, \ldots, m$, where $\varphi_0 < \varphi_1 < \cdots < \varphi_m < \varphi_{m+1} = b$. Here, φ denotes the current variable, ϖ denotes the outer integration variable, and ω denotes the inner integration variable. The Volterra term is integrated over $[\varphi_0, \varpi]$, whereas the Fredholm term is integrated over the fixed interval $[\varphi_0, b]$. The impulse operators act directly on the state variable ψ, rather than on the neutral variable $y(\varphi) = \psi(\varphi) - \xi_1(\varphi, \psi(\varphi))$. Only the impulses occurring before the current time φ are included in the summation.

Proof. If $\varphi \in (0, \varphi_1]$, we have the following problem:

$$\begin{aligned}
{}^{C}D^{\aleph}\Big[\psi(\varphi) - \xi_1(\varphi, \psi(\varphi))\Big] = {} & \Upsilon(\varphi)\psi(\varphi) + \xi_2(\varphi, \psi(\varphi)) + \int_{\varphi_0}^{\varphi} \zeta_1(\varphi, \varpi, \psi(\varpi))d\varpi \\
& + \int_{\varphi_0}^{b} \zeta_2(\varphi, \varpi, \psi(\varpi))d\varpi, \\
\psi(\varphi_0) = {} & \psi_0.
\end{aligned}$$

By applying the integral operator to both sides of the equation, we obtain the solution as

$$\begin{aligned}\psi(\varphi) - \psi_{\varphi_0} + \xi_1(\varphi_0, \psi_0) - \xi_1(\varphi, \psi(\varphi)) &= \frac{1}{\Gamma(\aleph)} \int_{\varphi_0}^{\varphi} (\varphi - \varpi)^{\aleph-1} \Upsilon(\varpi)\psi(\varpi) d\varpi \\ &+ \frac{1}{\Gamma(\aleph)} \int_{\varphi_0}^{\varphi} (\varphi - \varpi)^{\aleph-1} \xi_2(\varpi, \psi(\varpi)) d\varpi \\ &+ \frac{1}{\Gamma(\aleph)} \int_{\varphi_0}^{\varphi} (\varphi - \varpi)^{\aleph-1} \int_{\varphi_0}^{\varpi} \zeta_1(\varpi, \omega, \psi(\omega))\, d\omega\, d\varpi \\ &+ \frac{1}{\Gamma(\aleph)} \int_{\varphi_0}^{\varphi} (\varphi - \varpi)^{\aleph-1} \int_{\varphi_0}^{b} \zeta_2(\varpi, \omega, \psi(\omega))\, d\omega\, d\varpi,\end{aligned}$$

$$\begin{aligned}\psi(\varphi) = \psi_0 - \xi_1(\varphi_0, \psi_0) + \xi_1(\varphi, \psi(\varphi)) &+ \frac{1}{\Gamma(\aleph)} \int_{\varphi_0}^{\varphi} (\varphi - \varpi)^{\aleph-1} \Upsilon(\varpi)\psi(\varpi) d\varpi \\ &+ \frac{1}{\Gamma(\aleph)} \int_{\varphi_0}^{\varphi} (\varphi - \varpi)^{\aleph-1} \xi_2(\varpi, \psi(\varpi)) d\varpi \\ &+ \frac{1}{\Gamma(\aleph)} \int_{\varphi_0}^{\varphi} (\varphi - \varpi)^{\aleph-1} \int_{\varphi_0}^{\varpi} \zeta_1(\varpi, \omega, \psi(\omega))\, d\omega\, d\varpi \\ &+ \frac{1}{\Gamma(\aleph)} \int_{\varphi_0}^{\varphi} (\varphi - \varpi)^{\aleph-1} \int_{\varphi_0}^{b} \zeta_2(\varpi, \omega, \psi(\omega))\, d\omega\, d\varpi.\end{aligned}$$

If $\varphi \in (\varphi_k, \varphi_{k+1}]$, $k = 1, 2, \ldots, m$, we have the following equations:

$$\begin{aligned}{}^{C}D^{\aleph}\Big[\psi(\varphi) - \xi_1(\varphi, \psi(\varphi))\Big] &= \Upsilon(\varphi)\psi(\varphi) + \xi_2(\varphi, \psi(\varphi)) + \int_{\varphi_0}^{\varphi} \zeta_1(\varphi, \varpi, \psi(\varpi)) d\varpi \\ &+ \int_{\varphi_0}^{b} \zeta_2(\varphi, \varpi, \psi(\varpi)) d\varpi, \\ \psi(\varphi_k^+) &= \psi(\varphi_k^-) + I_k(\psi(\varphi_k^-)).\end{aligned}$$

Evidently, the above equations can be demonstrated as follows by applying the operator on the right-hand side of Eq (3.1) and using the operator. The resultant solution is given by the equation defined by (3.3). □

Theorem 3.1. Assuming that conditions $(B1)$–$(B6)$ are satisfied, we can assert that Eqs (3.1)–(3.2) have at least one solution.

Proof. Let $\Lambda_\gamma = \{\psi \in PC(\mathcal{J}; \mathcal{X}) : \|\psi\|_\infty \leq \gamma\}$. Then Λ_γ is a nonempty, closed, and convex subset of $PC(\mathcal{J}; \mathcal{X})$. The operator formulation of the integral equation (3.3) is given by:

$$\begin{aligned}(\vartheta\psi)(\varphi) = \psi_0 - \xi_1(\varphi_0, \psi_0) + \xi_1(\varphi, \psi(\varphi)) &+ \frac{1}{\Gamma(\aleph)} \int_{\varphi_0}^{\varphi} (\varphi - \varpi)^{\aleph-1} \Upsilon(\varpi)\psi(\varpi) d\varpi \\ &+ \frac{1}{\Gamma(\aleph)} \int_{\varphi_0}^{\varphi} (\varphi - \varpi)^{\aleph-1} \xi_2(\varpi, \psi(\varpi)) d\varpi \\ &+ \frac{1}{\Gamma(\aleph)} \int_{\varphi_0}^{\varphi} (\varphi - \varpi)^{\aleph-1} \left[\int_{\varphi_0}^{\varpi} \zeta_1(\varpi, \omega, \psi(\omega))\, d\omega + \int_{\varphi_0}^{b} \zeta_2(\varpi, \omega, \psi(\omega))\, d\omega\right] d\varpi \\ &+ \sum_{\varphi_k < \varphi} I_k(\psi(\varphi_k^-)).\end{aligned}$$

Initially, we observe that the operator ϑ is self-mapping. To illustrate this property, let φ be an element of the set $\mathcal{J}$ and ψ be an element of the set Λ_γ. Consequently, it follows that:

$$
\begin{aligned}
|(\vartheta\psi)(\varphi)| &\leq |\psi_0| + |\xi_1(\varphi_0,\psi_0)| + |\xi_1(\varphi,\psi(\varphi))| + \frac{1}{\Gamma(\aleph)}\int_{\varphi_0}^{\varphi}(\varphi-\varpi)^{\aleph-1}|\Upsilon(\varpi)||\psi(\varpi)|d\varpi \\
&\quad + \frac{1}{\Gamma(\aleph)}\int_{\varphi_0}^{\varphi}(\varphi-\varpi)^{\aleph-1}|\xi_2(\varpi,\ \psi(\varpi))|d\varpi \\
&\quad + \frac{1}{\Gamma(\aleph)}\int_{\varphi_0}^{\varphi}(\varphi-\varpi)^{\aleph-1}\Big(\int_{\varphi_0}^{\varpi}|\zeta_1(\varpi,\omega,\psi(\omega))|\,d\omega + \int_{\varphi_0}^{b}|\zeta_2(\varpi,\omega,\psi(\omega))|\,d\omega\Big)d\varpi \\
&\quad + \sum_{k=1}^{m}|I_k(\psi(\varphi_k^-))| \\
&\leq |\psi_0| + |\xi_1(\varphi_0,\psi_0)| + |\xi_1(\varpi,\psi(\varpi)) - \xi_1(\varpi,0)| + |\xi_1(\varpi,0)| \\
&\quad + \frac{1}{\Gamma(\aleph)}\int_{\varphi_0}^{\varphi}(\varphi-\varpi)^{\aleph-1}\|\Upsilon\|_\infty\|\psi\|_\infty d\varpi \\
&\quad + \frac{1}{\Gamma(\aleph)}\int_{\varphi_0}^{\varphi}(\varphi-\varpi)^{\aleph-1}(|\xi_2(\varpi,\ \psi(\varpi)) - \xi_2(\varpi,\ 0)| + |\xi_2(\varpi,\ 0)|)d\varpi \\
&\quad + \frac{1}{\Gamma(\aleph)}\int_{\varphi_0}^{\varphi}(\varphi-\varpi)^{\aleph-1}\Big(\int_{\varphi_0}^{\varpi}(|\zeta_1(\varpi,\omega,\psi(\omega)) - \zeta_1(\varpi,\omega,0)| + |\zeta_1(\varpi,\omega,0)|)\,d\omega \\
&\quad + \int_{\varphi_0}^{b}(|\zeta_2(\varpi,\omega,\psi(\omega)) - \zeta_2(\varpi,\omega,0)| + |\zeta_2(\varpi,\omega,0)|)\,d\omega\Big)d\varpi + m\lambda_2^* \\
&\leq |\psi_0| + |\xi_1(\varphi_0,\psi_0)| + (L_{\xi_1} + L_{\xi_1}^*\gamma) + \frac{\|\Upsilon\|_\infty b^{\aleph}\gamma}{\Gamma(\aleph+1)} + \frac{b^{\aleph}}{\Gamma(\aleph+1)}(L_{\xi_2}\gamma + L_{\xi_2}^*) \\
&\quad + \frac{b^{(\aleph+1)}}{(\aleph+1)\Gamma(\aleph)}(L_{\zeta_1}\gamma + L_{\zeta_1}^*) + \frac{b^{(\aleph+1)}}{(\aleph+1)\Gamma(\aleph)}(L_{\zeta_2}\gamma + L_{\zeta_2}^*) + m\lambda_2^*
\end{aligned}
$$

$$
\begin{aligned}
&\leq |\psi_0| + |\xi_1(\varphi_0,\psi_0)| + (L_{\xi_1}\gamma + L_{\xi_1}^*) + b^{\aleph}\Big(\frac{L_{\xi_2}^*}{\Gamma(\aleph+1)} + \frac{(L_{\zeta_1}^* + L_{\zeta_2}^*)b}{(\aleph+1)\Gamma(\aleph)}\Big) \\
&\quad + b^{\aleph}\gamma\Big(\frac{\|\Upsilon\|_\infty + L_{\xi_2}}{\Gamma(\aleph+1)} + \frac{(L_{\zeta_1} + L_{\zeta_2})b}{(\aleph+1)\Gamma(\aleph)}\Big) + m\lambda_2^*, \\
|(\vartheta\psi)(\varphi) - \psi_0| &\leq |\xi_1(\varphi_0,\psi_0)| + L_{\xi_1}\gamma + L_{\xi_1}^* + b^{\aleph}\Big(\frac{L_{\xi_2}^*}{\Gamma(\aleph+1)} + \frac{(L_{\zeta_1}^* + L_{\zeta_2}^*)b}{(\aleph+1)\Gamma(\aleph)}\Big) \\
&\quad + m\lambda_2^* + b^{\aleph}\gamma\Big(\frac{\|\Upsilon\|_\infty + L_{\xi_2}}{\Gamma(\aleph+1)} + \frac{(L_{\zeta_1} + L_{\zeta_2})b}{(\aleph+1)\Gamma(\aleph)}\Big) = \mathfrak{L}.
\end{aligned}
$$

We have established that ϑ maps the set $\Lambda_\gamma = \psi \in PC(\mathcal{J};\mathcal{X}) : |\psi|\infty \leq \gamma$ onto itself.

Next, we will show that the operator $\vartheta : \Lambda\gamma \to \Lambda_\gamma$ meets all the conditions specified in (2.2). The proof will be conducted in several stages.

Step 1. The operator ϑ is continuous.

Let ψ_n be a sequence such that $\psi_n \to \psi$ in Λ_γ. Then,

$$\begin{aligned}
|(\vartheta\psi_n)(\varphi) - (\vartheta\psi)(\varphi)| &\leq |\xi_1(\varphi, \psi_n(\varphi)) - \xi_1(\varphi, \psi(\varphi))| \\
&\quad + \frac{1}{\Gamma(\aleph)} \int_{\varphi_0}^{\varphi} (\varphi - \varpi)^{\aleph-1} |\Upsilon(\varpi)| \|\psi_n(\varpi) - \psi(\varpi)| \, d\varpi \\
&\quad + \frac{1}{\Gamma(\aleph)} \int_{\varphi_0}^{\varphi} (\varphi - \varpi)^{\aleph-1} |\xi_2(\varpi, \psi_n(\varpi)) - \xi_2(\varpi, \psi(\varpi))| \, d\varpi \\
&\quad + \frac{1}{\Gamma(\aleph)} \int_{\varphi_0}^{\varphi} (\varphi - \varpi)^{\aleph-1} \Big(\int_{\varphi_0}^{\varpi} |\zeta_1(\varpi, \omega, \psi_n(\omega)) - \zeta_1(\varpi, \omega, \psi(\omega))| \, d\omega \\
&\qquad\qquad + \int_{\varphi_0}^{b} |\zeta_2(\varpi, \omega, \psi_n(\omega)) - \zeta_2(\varpi, \omega, \psi(\omega))| \, d\omega \Big) d\varpi \\
&\quad + \sum_{\varphi_k < \varphi} |I_k(\psi_n(\varphi_k^-)) - I_k(\psi(\varphi_k^-))| \\
&\leq L_{\xi_1} \|\psi_n(\varpi) - \psi(\varpi)\| + \frac{\|\Upsilon\|_\infty b^{\aleph}}{\Gamma(\aleph + 1)} \|\psi_n(\varpi) - \psi(\varpi)\| + \frac{L_{\xi_2} b^{\aleph}}{\Gamma(\aleph + 1)} \|\psi_n(\varpi) - \psi(\varpi)\| \\
&\quad + \frac{L_{\zeta_1} b^{\aleph+1} + L_{\zeta_2} b^{\aleph+1}}{(\aleph + 1)\Gamma(\aleph)} \|\psi_n(\varpi) - \psi(\varpi)\| + m\lambda_1^* \|\psi_n(\varpi) - \psi(\varpi)\| \\
&= \left(L_{\xi_1} + \frac{\|\Upsilon\|_\infty + L_{\xi_2}}{\Gamma(\aleph + 1)} + \frac{(L_{\zeta_1} + L_{\zeta_2}) b}{(\aleph + 1)\Gamma(\aleph)} \right) b^{\aleph} + m\lambda_1^* \|\psi_n(\varpi) - \psi(\varpi)\|.
\end{aligned}$$

Because ξ, ζ_1, and ζ_2 are continuous, it follows that:

$$\|(\vartheta\psi_n)(\varphi) - (\vartheta\psi)(\varphi)\| \to 0 \text{ as } n \to \infty.$$

Therefore, ϑ is continuous on the set Λ_γ.

Step 2. The set $\vartheta(\Lambda_\gamma)$ is uniformly bounded. This is clear since $\vartheta(\Lambda_\gamma) \subset \Lambda_\gamma$, which implies it is bounded.

Step 3. We need to show that $\vartheta(\Lambda_\gamma)$ is equicontinuous.

Fix $k \in \{0, 1, \ldots, m\}$ and consider $\varphi_1, \varphi_2 \in (\varphi_k, \varphi_{k+1}]$ with $\varphi_1 < \varphi_2$. Since there is no impulsive point in $(\varphi_1, \varphi_2]$, the impulse contributions in $(\vartheta\psi)(\varphi_2)$ and $(\vartheta\psi)(\varphi_1)$ are identical and therefore cancel. For $\psi \in \Lambda_\gamma$, we have

$$\begin{aligned}
\|(\vartheta\psi)(\varphi_2) - (\vartheta\psi)(\varphi_1)\| &\leq \|\xi_1(\varphi_2, \psi(\varphi_2)) - \xi_1(\varphi_1, \psi(\varphi_1))\| \\
&\quad + \frac{1}{\Gamma(\aleph)} \Big\| \int_{\varphi_0}^{\varphi_2} (\varphi_2 - \varpi)^{\aleph-1} \Upsilon(\varpi)\psi(\varpi) \, d\varpi \\
&\qquad\qquad - \int_{\varphi_0}^{\varphi_1} (\varphi_1 - \varpi)^{\aleph-1} \Upsilon(\varpi)\psi(\varpi) \, d\varpi \Big\| \\
&\quad + \frac{1}{\Gamma(\aleph)} \Big\| \int_{\varphi_0}^{\varphi_2} (\varphi_2 - \varpi)^{\aleph-1} \xi_2(\varpi, \psi(\varpi)) \, d\varpi \\
&\qquad\qquad - \int_{\varphi_0}^{\varphi_1} (\varphi_1 - \varpi)^{\aleph-1} \xi_2(\varpi, \psi(\varpi)) \, d\varpi \Big\| \\
&\quad + \frac{1}{\Gamma(\aleph)} \Big\| \int_{\varphi_0}^{\varphi_2} (\varphi_2 - \varpi)^{\aleph-1} \Big[\int_{\varphi_0}^{\varpi} \zeta_1(\varpi, \omega, \psi(\omega)) \, d\omega
\end{aligned}$$

$$+\int_{\varphi_0}^{b}\zeta_2(\varpi,\omega,\psi(\omega))\,d\omega\Big]\,d\varpi$$
$$-\int_{\varphi_0}^{\varphi_1}(\varphi_1-\varpi)^{\aleph-1}\Big[\int_{\varphi_0}^{\varpi}\zeta_1(\varpi,\omega,\psi(\omega))\,d\omega$$
$$+\int_{\varphi_0}^{b}\zeta_2(\varpi,\omega,\psi(\omega))\,d\omega\Big]\,d\varpi\Big\|.$$

The first term tends to zero as $\varphi_2 \to \varphi_1$ by the continuity of ξ_1 and the continuity of ψ on each impulse-free interval. For the fractional integral terms, we split the integrals over $[\varphi_0, \varphi_2]$ into $[\varphi_0, \varphi_1]$ and $[\varphi_1, \varphi_2]$. Thus,

$$\begin{aligned}\|(\vartheta\psi)(\varphi_2)-(\vartheta\psi)(\varphi_1)\| &\le \|\xi_1(\varphi_2,\psi(\varphi_2))-\xi_1(\varphi_1,\psi(\varphi_1))\|\\
&\quad+\frac{1}{\Gamma(\aleph)}\Big\|\int_{\varphi_1}^{\varphi_2}(\varphi_2-\varpi)^{\aleph-1}\Upsilon(\varpi)\psi(\varpi)\,d\varpi\\
&\quad+\int_{\varphi_0}^{\varphi_1}\left[(\varphi_2-\varpi)^{\aleph-1}-(\varphi_1-\varpi)^{\aleph-1}\right]\Upsilon(\varpi)\psi(\varpi)\,d\varpi\Big\|\\
&\quad+\frac{1}{\Gamma(\aleph)}\Big\|\int_{\varphi_1}^{\varphi_2}(\varphi_2-\varpi)^{\aleph-1}\xi_2(\varpi,\psi(\varpi))\,d\varpi\\
&\quad+\int_{\varphi_0}^{\varphi_1}\left[(\varphi_2-\varpi)^{\aleph-1}-(\varphi_1-\varpi)^{\aleph-1}\right]\xi_2(\varpi,\psi(\varpi))\,d\varpi\Big\|\\
&\quad+\frac{1}{\Gamma(\aleph)}\Big\|\int_{\varphi_1}^{\varphi_2}(\varphi_2-\varpi)^{\aleph-1}\Big[\int_{\varphi_0}^{\varpi}\zeta_1(\varpi,\omega,\psi(\omega))\,d\omega\\
&\qquad+\int_{\varphi_0}^{b}\zeta_2(\varpi,\omega,\psi(\omega))\,d\omega\Big]\,d\varpi\\
&\quad+\int_{\varphi_0}^{\varphi_1}\left[(\varphi_2-\varpi)^{\aleph-1}-(\varphi_1-\varpi)^{\aleph-1}\right]\\
&\qquad\times\Big[\int_{\varphi_0}^{\varpi}\zeta_1(\varpi,\omega,\psi(\omega))\,d\omega+\int_{\varphi_0}^{b}\zeta_2(\varpi,\omega,\psi(\omega))\,d\omega\Big]\,d\varpi\Big\|.\end{aligned}$$

Using $\|\psi\|_\infty \le \gamma$, $\|\Upsilon\|_\infty < \infty$, and the boundedness of ξ_2, ζ_1, and ζ_2 on the corresponding bounded sets, the contributions over $[\varphi_1, \varphi_2]$ are bounded by

$$\frac{1}{\Gamma(\aleph)}\int_{\varphi_1}^{\varphi_2}(\varphi_2-\varpi)^{\aleph-1}\,d\varpi=\frac{(\varphi_2-\varphi_1)^{\aleph}}{\aleph\Gamma(\aleph)}\longrightarrow 0$$

as $\varphi_2 \to \varphi_1$, since $0 < \aleph \le 1$. The remaining integrals over $[\varphi_0, \varphi_1]$ tend to zero by the continuity of the fractional kernel with respect to φ and the dominated convergence theorem. Hence, all the fractional integral contributions tend to zero as $\varphi_2 \to \varphi_1$.

Moreover, because ξ_1, ξ_2, ζ_1, and ζ_2 satisfy the assumptions in $(B1)$–$(B4)$ and $\psi \in \Lambda_\gamma$, the above estimates are independent of the particular choice of $\psi \in \Lambda_\gamma$. Therefore,

$$\sup_{\psi\in\Lambda_\gamma}\|(\vartheta\psi)(\varphi_2)-(\vartheta\psi)(\varphi_1)\|\longrightarrow 0\qquad\text{as } \varphi_2\to\varphi_1,$$

for $\varphi_1, \varphi_2 \in (\varphi_k, \varphi_{k+1}]$. Thus, $\vartheta(\Lambda_\gamma)$ is equicontinuous on every impulse-free interval. At each impulsive point φ_k, the left and right limits are considered separately according to the definition of $PC(\mathcal{J}; X)$, and the prescribed impulse condition determines the corresponding jump.

Combining Steps 1–3 with the Banach-valued Arzelà–Ascoli theorem in Theorem 2.1 and the pointwise relative compactness assumption $(B6)$, we conclude that $\vartheta(\Lambda_\gamma)$ is relatively compact in $PC(\mathcal{J}; X)$. Hence, ϑ is a continuous and compact operator on Λ_γ. Therefore, by the Schauder fixed point theorem in Theorem 2.2, ϑ has a fixed point in Λ_γ, which is a solution of (3.1)–(3.2). This completes the proof of the theorem. □

4. Controllability results

In this section, we will demonstrate the controllability of the Caputo fractional impulsive neutral VFIDE with a particular form of control parameter:

$$\begin{aligned} {}^{C}D^{\aleph}\Big[\psi(\varphi) - \xi_1(\varphi, \psi(\varphi))\Big] = \Upsilon(\varphi)\psi(\varphi) + \xi_2(\varphi, \psi(\varphi)) + \int_{\varphi_0}^{\varphi} \zeta_1(\varphi, \varpi, \psi(\varpi))d\varpi \\ + \int_{\varphi_0}^{b} \zeta_2(\varphi, \varpi, \psi(\varpi))d\varpi + (Bu)(\varphi) \\ \Delta\psi(\varphi_k) = I_k(\psi(\varphi_k^-)). \end{aligned} \tag{4.1}$$

The equation is accompanied by the following initial condition:

$$\psi(\varphi_0) = \psi_0. \tag{4.2}$$

Given that the state variable $x(\cdot)$ is an element of the Banach space X, and the control function $\mu(\cdot)$ is situated in the Banach space $L^2(\mathcal{J}, U)$. where U is the underlying Banach space for allowable control functions, the operator B is a bounded linear map from U to X. Under these conditions, a mild solution to Eqs (4.1)–(4.2) exists and can be expressed as:

$$\begin{aligned} \psi(\varphi) = \psi_0 - \xi_1(\varphi_0, \psi_0) + \xi_1(\varphi, \psi(\varphi)) + \frac{1}{\Gamma(\aleph)} \int_{\varphi_0}^{\varphi} (\varphi - \varpi)^{\aleph-1} \Upsilon(\varpi)\psi(\varpi)d\varpi \\ + \frac{1}{\Gamma(\aleph)} \int_{\varphi_0}^{\varphi} (\varphi - \varpi)^{\aleph-1} \xi_2(\varpi, \psi(\varpi))d\varpi \\ + \frac{1}{\Gamma(\aleph)} \int_{\varphi_0}^{\varphi} (\varphi - \varpi)^{\aleph-1} \int_{\varphi_0}^{\varpi} \zeta_1(\varpi, \omega, \psi(\omega))\, d\omega\, d\varpi \\ + \frac{1}{\Gamma(\aleph)} \int_{\varphi_0}^{\varphi} (\varphi - \varpi)^{\aleph-1} \int_{\varphi_0}^{b} \zeta_2(\varpi, \omega, \psi(\omega))\, d\omega\, d\varpi \\ + \frac{1}{\Gamma(\aleph)} \int_{\varphi_0}^{\varphi} (\varphi - \varpi)^{\aleph-1} Bu(\varpi)d\varpi + \sum_{\varphi_k < \varphi} I_k(\psi(\varphi_k^-)) \end{aligned} \tag{4.3}$$

for $\varphi \in (\varphi_k, \varphi_{k+1}]$, $k = 1, 2, \ldots, m$.

Theorem 4.1. Under the fulfillment of hypotheses $(B1)-(B6)$, we introduce the additional assumption:

(*B*7) For each $\varphi \in \mathcal{J}$, define the partial control operator $W_\varphi : L^2(\mathcal{J}, U) \to \mathcal{X}$ by

$$W_\varphi u = \frac{1}{\Gamma(\aleph)} \int_{\varphi_0}^{\varphi} (\varphi - \varpi)^{\aleph-1} Bu(\varpi)\, d\varpi.$$

In particular, let $W = W_b$, where

$$Wu = \frac{1}{\Gamma(\aleph)} \int_{\varphi_0}^{b} (b - \varpi)^{\aleph-1} Bu(\varpi)\, d\varpi.$$

Since $\frac{1}{2} < \aleph \leq 1$, the kernel $(b-\varpi)^{\aleph-1}$ belongs to $L^2(\mathcal{J})$. Hence, by the Cauchy–Schwarz inequality, $W : L^2(\mathcal{J}, U) \to \mathcal{X}$ is bounded. In particular,

$$\|Wu\| \leq \frac{M_1}{\Gamma(\aleph)} \left(\int_{\varphi_0}^{b} (b - \varpi)^{2\aleph-2}\, d\varpi \right)^{1/2} \|u\|_{L^2(\mathcal{J},U)} = \frac{M_1 T^{\aleph-\frac{1}{2}}}{\Gamma(\aleph)\sqrt{2\aleph - 1}} \|u\|_{L^2(\mathcal{J},U)},$$

where $T = b - \varphi_0$. Therefore,

$$\|W\| \leq \frac{M_1 T^{\aleph-\frac{1}{2}}}{\Gamma(\aleph)\sqrt{2\aleph - 1}}.$$

Assume that W is surjective and admits a bounded right inverse $W^{-1} : \mathcal{X} \to L^2(\mathcal{J}, U)$ satisfying $WW^{-1} = I_{\mathcal{X}}$ and $\|W^{-1}\| \leq M_2$. Moreover, $B : U \to \mathcal{X}$ is bounded with $\|B\| \leq M_1$.

Proof. Let $\Lambda_{\gamma_1} = \{\psi \in PC(\mathcal{J}; \mathcal{X}) : \|\psi\|_\infty \leq \gamma_1\}$. For each $\psi \in \Lambda_{\gamma_1}$, we construct a control function from the prescribed terminal condition $\psi(b) = \psi_1$. Given the assumptions made in hypothesis (*B*5), a suitable control function can be established based on the characteristics of any function $\psi(.)$ within this set. Now we have

$$\begin{aligned}
\mu = W^{-1}\Bigg[& \psi_1 - \psi_0 + \xi_1(\varphi_0, \psi_0) - \xi_1(b, \psi(b)) \\
& - \frac{1}{\Gamma(\aleph)} \int_{\varphi_0}^{b} (b - \varpi)^{\aleph-1} \Bigg[\Upsilon(\varpi)\psi(\varpi) + \xi_2(\varpi, \psi(\varpi)) \\
& + \int_{\varphi_0}^{\varpi} \zeta_1(\varpi, \omega, \psi(\omega))\, d\omega + \int_{\varphi_0}^{b} \zeta_2(\varpi, \omega, \psi(\omega))\, d\omega \Bigg] d\varpi \\
& - \sum_{\varphi_k < b} I_k(\psi(\varphi_k^-)) \Bigg].
\end{aligned} \tag{4.4}$$

Utilizing the given control, we aim to show that the operator Ψ maps the set Λ_{γ_1} onto itself. The definition of the operator Ψ is as follows:

$$\begin{aligned}
(\Psi\psi)(\varphi) = & \psi_0 - \xi_1(\varphi_0, \psi_0) + \xi_1(\varphi, \psi(\varphi)) \\
& + \frac{1}{\Gamma(\aleph)} \int_{\varphi_0}^{\varphi} (\varphi - \varpi)^{\aleph-1} \Bigg[\Upsilon(\varpi)\psi(\varpi) + \xi_2(\varpi, \psi(\varpi)) \\
& + \int_{\varphi_0}^{\varpi} \zeta_1(\varpi, \omega, \psi(\omega))\, d\omega + \int_{\varphi_0}^{b} \zeta_2(\varpi, \omega, \psi(\omega))\, d\omega + B\mu(\varpi) \Bigg] d\varpi \\
& + \sum_{\varphi_k < \varphi} I_k(\psi(\varphi_k^-)).
\end{aligned} \tag{4.5}$$

The control function μ is defined by Eq (4.4). By the definition of μ and the relation $WW^{-1} = I_{\mathcal{X}}$, the terminal condition is satisfied at $\varphi = b$. Hence, if ψ is a fixed point of Ψ, then $(\Psi\psi)(b) = \psi_1$. Therefore, the corresponding fixed point provides a mild solution of (4.1)–(4.2) satisfying the prescribed initial and terminal conditions.

To prove the continuity of Ψ, let $\{\psi_n\}$ be a sequence in Λ_{γ_1} such that $\psi_n \to \psi$ in Λ_{γ_1}. By the continuity assumptions on $\xi_1, \xi_2, \zeta_1, \zeta_2$, and the boundedness of B and W^{-1}, together with the dominated convergence theorem, the corresponding control functions defined by (4.4) satisfy

$$\|\mu_n - \mu\|_{L^2(\mathcal{J},U)} \longrightarrow 0.$$

Consequently, from (4.5),

$$\|\Psi\psi_n - \Psi\psi\|_\infty \longrightarrow 0.$$

Hence, $\Psi : \Lambda_{\gamma_1} \to \Lambda_{\gamma_1}$ is continuous.

Applying Eq (4.3), for any function ψ belonging to the set Λ_{γ_1} and for all φ in the interval $[\varphi_0, b]$, we can derive the following relationship:

$$\begin{aligned}
\|\mu(\varphi)\| \le \|W^{-1}\|\Big[&\|\psi_1\| + \|\psi_0\| + \|\xi_1(\varphi_0,\psi_0)\| + (L_{\xi_1} + L^*_{\xi_1}\gamma_1) \\
&+ \frac{\|\Upsilon\|_\infty b^{\aleph}\gamma_1}{\Gamma(\aleph+1)} + \frac{b^{\aleph}}{\Gamma(\aleph+1)}(L_{\xi_2}\gamma_1 + L^*_{\xi_2}) + \frac{b^{(\aleph+1)}}{(\aleph+1)\Gamma(\aleph)}(L_{\zeta_1}\gamma_1 + L^*_{\zeta_1}) \\
&+ \frac{b^{(\aleph+1)}}{(\aleph+1)\Gamma(\aleph)}(L_{\zeta_2}\gamma_1 + L^*_{\zeta_2}) + m\lambda_2^*\Big], \\
\|\mu(\varphi)\| \le M_2\Big[&\|\psi_1\| + \|\psi_0\| + \|\xi_1(\varphi_0,\psi_0)\| + (L_{\xi_1} + L^*_{\xi_1}\gamma_1) \\
&+ \frac{\|\Upsilon\|_\infty b^{\aleph}\gamma_1}{\Gamma(\aleph+1)} + \frac{b^{\aleph}}{\Gamma(\aleph+1)}(L_{\xi}\gamma_1 + L^*_{\xi}) + \frac{b^{(\aleph+1)}}{(\aleph+1)\Gamma(\aleph)}(L_{\zeta_1}\gamma_1 + L^*_{\zeta_1}) \\
&+ \frac{b^{(\aleph+1)}}{(\aleph+1)\Gamma(\aleph)}(L_{\zeta_2}\gamma_1 + L^*_{\zeta_2}) + m\lambda_2^*\Big].
\end{aligned} \tag{4.6}$$

Using Eq (4.6), we can obtain the following result:

$$\begin{aligned}
\|\Psi\psi(\varphi)\| &\le \|\psi_0\| + \|\xi_1(\varphi_0,\psi_0)\| + (L_{\xi_1} + L^*_{\xi_1}\gamma_1) + \frac{\|\Upsilon\|_\infty b^{\aleph}\gamma_1}{\Gamma(\aleph+1)} \\
&+ \frac{b^{\aleph}}{\Gamma(\aleph+1)}(L_{\xi_2}\gamma_1 + L^*_{\xi_2}) + \frac{b^{(\aleph+1)}}{(\aleph+1)\Gamma(\aleph)}(L_{\zeta_1}\gamma_1 + L^*_{\zeta_1}) \\
&+ \frac{b^{(\aleph+1)}}{(\aleph+1)\Gamma(\aleph)}(L_{\zeta_2}\gamma_1 + L^*_{\zeta_2}) + \frac{b^{\aleph}}{\Gamma(\aleph+1)}M_1\|\mu(\varphi)\| + m\lambda_2^* \\
&\le \|\psi_0\| + \|\xi_1(\varphi_0,\psi_0)\| + (L_{\xi_1} + L^*_{\xi_1}\gamma_1) + \frac{\|\Upsilon\|_\infty b^{\aleph}\gamma_1}{\Gamma(\aleph+1)} + \frac{b^{\aleph}}{\Gamma(\aleph+1)}(L_{\xi_2}\gamma_1 + L^*_{\xi_2}) \\
&+ \frac{b^{(\aleph+1)}}{(\aleph+1)\Gamma(\aleph)}(L_{\zeta_1}\gamma_1 + L^*_{\zeta_1}) + \frac{b^{(\aleph+1)}}{(\aleph+1)\Gamma(\aleph)}(L_{\zeta_2}\gamma_1 + L^*_{\zeta_2}) + m\lambda_2^* \\
&+ \frac{b^{\aleph}}{\Gamma(\aleph+1)}M_1\Big[M_2\|\psi_1\| + M_2\|\psi_0\| + M_2\|\xi_1(\varphi_0,\psi_0)\| \\
&+ M_2(L_{\xi_1} + L^*_{\xi_1}\gamma_1) + M_2\frac{\|\Upsilon\|_\infty b^{\aleph}\gamma_1}{\Gamma(\aleph+1)}
\end{aligned}$$

$$
\begin{aligned}
&+ M_2\frac{b^{\aleph}}{\Gamma(\aleph+1)}(L_{\xi_2}\gamma_1 + L^*_{\xi_2}) + M_2\frac{b^{(\aleph+1)}}{(\aleph+1)\Gamma(\aleph)}(L_{\zeta_1}\gamma_1 + L^*_{\zeta_1})\\
&+ M_2\frac{b^{(\aleph+1)}}{(\aleph+1)\Gamma(\aleph)}(L_{\zeta_2}\gamma_1 + L^*_{\zeta_2}) + M_2 m\lambda^*_2\Big]\\
&\leq \frac{b^{\aleph}}{\Gamma(\aleph+1)}M_1M_2\|\psi_1\| + \Big(1 + \frac{b^{\aleph}}{\Gamma(\aleph+1)}M_1M_2\Big)\|\psi_0\|\\
&+ \|\xi_1(\varphi_0,\psi_0)\|(1 + M_1M_2)\\
&+ (1 + M_1M_2)(L_{\xi_1} + L^*_{\xi_1}\gamma_1) + \frac{\|\Upsilon\|_\infty b^{\aleph}\gamma_1}{\Gamma(\aleph+1)}\Big(1 + \frac{b^{\aleph}}{\Gamma(\aleph+1)}M_1M_2\Big)\\
&+ \frac{b^{\aleph}}{\Gamma(\aleph+1)}(L_{\xi_2}\gamma_1 + L^*_{\xi_2})\Big(1 + \frac{b^{\aleph}}{\Gamma(\aleph+1)}M_1M_2\Big)\\
&+ \frac{b^{(\aleph+1)}}{(\aleph+1)\Gamma(\aleph)}(L_{\zeta_1}\gamma_1 + L^*_{\zeta_1})\Big(1 + \frac{b^{\aleph}}{\Gamma(\aleph+1)}M_1M_2\Big)\\
&+ \frac{b^{(\aleph+1)}}{(\aleph+1)\Gamma(\aleph)}(L_{\zeta_2}\gamma_1 + L^*_{\zeta_2})\Big(1 + \frac{b^{\aleph}}{\Gamma(\aleph+1)}M_1M_2\Big) + M_1M_2m\lambda^*_2\\
&\leq \frac{b^{\aleph}}{\Gamma(\aleph+1)}M_1M_2\|\psi_1\| + \Big(1 + \frac{b^{\aleph}}{\Gamma(\aleph+1)}M_1M_2\Big)\Big[\|\psi_0\|\\
&+ \frac{\|\Upsilon\|_\infty b^{\aleph}\gamma_1}{\Gamma(\aleph+1)} + \frac{b^{\aleph}}{\Gamma(\aleph+1)}(L_{\xi_2}\gamma_1 + L^*_{\xi_2})\\
&+ \frac{b^{(\aleph+1)}}{(\aleph+1)\Gamma(\aleph)}(L_{\zeta_1}\gamma_1 + L^*_{\zeta_1}) + \frac{b^{(\aleph+1)}}{(\aleph+1)\Gamma(\aleph)}(L_{\zeta_2}\gamma_1 + L^*_{\zeta_2})\Big]\\
&+ \Big(\|\xi_1(\varphi_0,\psi_0)\| + (L_{\xi_1} + L^*_{\xi_1}\gamma_1)\Big)(1 + M_1M_2) + M_1M_2m\lambda^*_2\\
&\leq \mathfrak{Q}_1.
\end{aligned}
$$

This shows that the operator Ψ maps the set $\Lambda_{\gamma_1} = \{\psi \in PC(\mathcal{J};\mathcal{X}) : \|\psi\|_\infty \leq \gamma_1\}$ onto itself. We will now proceed to verify that the operator $\Psi : \Lambda_{\gamma_1} \to \Lambda_{\gamma_1}$ satisfies all the conditions of Theorem 2.2. The proof will be carried out in several steps.

Step 1. The operator Ψ is continuous. Let ψ_n be a sequence such that $\psi_n \to \psi$ in Λ_{γ_1}.

$$
\begin{aligned}
|(\Psi\psi_n)(\varphi) - (\Psi\psi)(\varphi)| \leq\ & |\xi_1(\varphi,\psi_n(\varphi)) - \xi_1(\varphi,\psi(\varphi))|\\
&+ \frac{1}{\Gamma(\aleph)}\int_{\varphi_0}^{\varphi}(\varphi-\varpi)^{\aleph-1}|\Upsilon(\varpi)||\psi_n(\varpi) - \psi(\varpi)|d\varpi\\
&+ \frac{1}{\Gamma(\aleph)}\int_{\varphi_0}^{\varphi}(\varphi-\varpi)^{\aleph-1}|\xi_2(\varpi,\psi_n(\varpi)) - \xi_2(\varpi,\psi(\varpi))|d\varpi\\
&+ \frac{1}{\Gamma(\aleph)}\int_{\varphi_0}^{\varphi}(\varphi-\varpi)^{\aleph-1}\Big(\int_{\varphi_0}^{\varpi}|\zeta_1(\varpi,\omega,\psi_n(\omega)) - \zeta_1(\varpi,\omega,\psi(\omega))|d\omega\\
&+ \int_{\varphi_0}^{b}|\zeta_2(\varpi,\omega,\psi_n(\omega)) - \zeta_2(\varpi,\omega,\psi(\omega))|d\omega\Big)d\varpi\\
&+ \sum_{\varphi_k<\varphi}|I_k(\psi_n(\varphi_k^-)) - I_k(\psi(\varphi_k^-))|
\end{aligned}
$$

$$
\begin{aligned}
&+ \frac{1}{\Gamma(\aleph)} \int_{\varphi_0}^{\varphi} (\varphi - \varpi)^{\aleph-1} BW^{-1}\Big[|\xi_1(\varphi, \psi_n(\varphi)) - \xi_1(\varphi, \psi(\varphi))| \\
&- \frac{1}{\Gamma(\aleph)} \int_{\varphi_0}^{b} (b - \varpi)^{\aleph-1}\Big[\Upsilon(\varpi)|\psi_n(\varpi) - \psi(\varpi)| \\
&+ |\xi_2(\varpi, \psi_n(\varpi)) - \xi_2(\varpi, \psi(\varpi))| \\
&+ \int_{\varphi_0}^{\varpi} |\zeta_1(\varpi, \omega, \psi_n(\omega)) - \zeta_1(\varpi, \omega, \psi(\omega))| d\omega \\
&+ \int_{\varphi_0}^{b} |\zeta_2(\varpi, \omega, \psi_n(\omega)) - \zeta_2(\varpi, \omega, \psi(\omega))| d\omega\Big] d\varpi \\
&+ \sum_{k=1}^{m} |I_k(\psi_n(\varphi_k^-)) - I_k(\psi(\varphi_k^-))|\Big].
\end{aligned}
$$

Given the continuity of ξ, ζ_1, and ζ_2, it can be deduced that:

$$\|(\Psi\psi_n)(\varphi) - (\Psi\psi)(\varphi)\| \to 0 \text{ as } n \to \infty.$$

Therefore, the operator Ψ is continuous on the set Λ_{γ_1}.

Step 2. The set $\vartheta(\Lambda_{\gamma_1})$ is uniformly bounded. This is clear since $\vartheta(\Lambda_{\gamma_1}) \subset \Lambda_{\gamma_1}$, which implies it is bounded.

Moreover, by assumption $(B6)$, for every fixed $\varphi \in \mathcal{J}$, the set

$$\Big\{(\vartheta\psi)(\varphi) : \psi \in \Lambda_{\gamma_1}\Big\}$$

is relatively compact in $\mathcal{X}$. Hence, $\vartheta(\Lambda_{\gamma_1})$ satisfies the pointwise relative compactness condition required by the Banach-valued Arzelà–Ascoli theorem.

Step 3. We show that $\Psi(\Lambda_{\gamma_1})$ is equicontinuous on each interval $(\varphi_k, \varphi_{k+1}]$, where $k = 0, 1, \ldots, m$. Let $\varphi_1, \varphi_2 \in (\varphi_k, \varphi_{k+1}]$ with $\varphi_1 < \varphi_2$ and let $\psi \in \Lambda_{\gamma_1}$. Since $\varphi_1, \varphi_2 \in (\varphi_k, \varphi_{k+1}]$, no impulsive point lies between φ_1 and φ_2. Hence, the impulsive contributions in $(\Psi\psi)(\varphi_2)$ and $(\Psi\psi)(\varphi_1)$ are identical and cancel in their difference.

$$
\begin{aligned}
\|(\Psi\psi)(\varphi_2) - (\Psi\psi)(\varphi_1)\| = \Big\|&\psi_0 - \xi_1(\varphi_0, \psi_0) + \xi_1(\varphi_2, \psi(\varphi_2)) \\
&+ \frac{1}{\Gamma(\aleph)} \int_{\varphi_0}^{\varphi_2} (\varphi_2 - \varpi)^{\aleph-1} \Upsilon(\varpi)\psi(\varpi) d\varpi \\
&+ \frac{1}{\Gamma(\aleph)} \int_{\varphi_0}^{\varphi_2} (\varphi_2 - \varpi)^{\aleph-1} \xi_2(\varpi, \psi(\varpi)) d\varpi \\
&+ \frac{1}{\Gamma(\aleph)} \int_{\varphi_0}^{\varphi_2} (\varphi_2 - \varpi)^{\aleph-1} \int_{\varphi_0}^{\varpi} \zeta_1(\varpi, \omega, \psi(\omega)) d\omega\, d\varpi \\
&+ \frac{1}{\Gamma(\aleph)} \int_{\varphi_0}^{\varphi_2} (\varphi_2 - \varpi)^{\aleph-1} \int_{\varphi_0}^{b} \zeta_2(\varpi, \omega, \psi(\omega)) d\omega\, d\varpi \\
&+ BW^{-1}\Big[\psi_1 - \psi_0 + \xi_1(\varphi_0, \psi_0) - \xi_1(\varphi_2, \psi(\varphi_2))
\end{aligned}
$$

$$
\begin{aligned}
&- \frac{1}{\Gamma(\aleph)} \int_{\varphi_0}^{\varphi_2} (\varphi_2 - \varpi)^{\aleph-1} \Big[\Upsilon(\varpi)\psi(\varpi) + \xi_2(\varpi, \psi(\varpi)) \\
&\quad + \int_{\varphi_0}^{\varpi} \zeta_1(\varpi, \omega, \psi(\omega)) d\omega + \int_{\varphi_0}^{b} \zeta_2(\varpi, \omega, \psi(\omega)) d\omega \Big] d\varpi \Big] \\
&- \psi_0 + \xi_1(\varphi_0, \psi_0) - \xi_1(\varphi_1, \psi(\varphi_1)) \\
&- \frac{1}{\Gamma(\aleph)} \int_{\varphi_0}^{\varphi_1} (\varphi_1 - \varpi)^{\aleph-1} \Upsilon(\varpi)\psi(\varpi) d\varpi \\
&- \frac{1}{\Gamma(\aleph)} \int_{\varphi_0}^{\varphi_1} (\varphi_1 - \varpi)^{\aleph-1} \xi_2(\varpi, \psi(\varpi)) d\varpi \\
&- \frac{1}{\Gamma(\aleph)} \int_{\varphi_0}^{\varphi_1} (\varphi_1 - \varpi)^{\aleph-1} \int_{\varphi_0}^{\varpi} \zeta_1(\varpi, \omega, \psi(\omega)) d\omega \, d\varpi \\
&- \frac{1}{\Gamma(\aleph)} \int_{\varphi_0}^{\varphi_1} (\varphi_1 - \varpi)^{\aleph-1} \int_{\varphi_0}^{b} \zeta_2(\varpi, \omega, \psi(\omega)) d\omega \, d\varpi \\
&- BW^{-1} \Big[\psi_1 - \psi_0 + \xi_1(\varphi_0, \psi_0) - \xi_1(\varphi_1, \psi(\varphi_1)) \\
&\quad - \frac{1}{\Gamma(\aleph)} \int_{\varphi_0}^{\varphi_1} (\varphi_1 - \varpi)^{\aleph-1} \Big[\Upsilon(\varpi)\psi(\varpi) + \xi_2(\varpi, \psi(\varpi)) \\
&\quad + \int_{\varphi_0}^{\varpi} \zeta_1(\varpi, \omega, \psi(\omega)) d\omega + \int_{\varphi_0}^{b} \zeta_2(\varpi, \omega, \psi(\omega)) d\omega \Big] d\varpi \Big] \Big\| \\
\leq\ & \frac{1}{\Gamma(\aleph)} \Big\| \int_{\varphi_1}^{\varphi_2} (\varphi_2 - \varpi)^{\aleph-1} \Big[\Upsilon(\varpi)\psi(\varpi) + \xi_2(\varpi, \psi(\varpi)) \\
&+ \int_{\varphi_0}^{\varpi} \zeta_1(\varpi, \omega, \psi(\omega)) \, d\omega + \int_{\varphi_0}^{b} \zeta_2(\varpi, \omega, \psi(\omega)) \, d\omega \Big] d\varpi \\
&- \int_{\varphi_0}^{\varphi_1} [(\varphi_1 - \varpi)^{\aleph-1} - (\varphi_2 - \varpi)^{\aleph-1}] \Upsilon(\varpi)\psi(\varpi) d\varpi \\
&- \int_{\varphi_0}^{\varphi_1} [(\varphi_1 - \varpi)^{\aleph-1} - (\varphi_2 - \varpi)^{\aleph-1}] \xi_2(\varpi, \psi(\varpi)) d\varpi \\
&- \int_{\varphi_0}^{\varphi_1} \Big[(\varphi_1 - \varpi)^{\aleph-1} \int_{\varphi_0}^{\varpi} \zeta_1(\varpi, \omega, \psi(\omega)) \, d\omega - (\varphi_2 - \varpi)^{\aleph-1} \int_{\varphi_0}^{\varpi} \zeta_1(\varpi, \omega, \psi(\omega)) \, d\omega \Big] d\varpi \\
&- \int_{\varphi_0}^{\varphi_1} \Big[(\varphi_1 - \varpi)^{\aleph-1} \int_{\varphi_0}^{b} \zeta_2(\varpi, \omega, \psi(\omega)) \, d\omega - (\varphi_2 - \varpi)^{\aleph-1} \int_{\varphi_0}^{b} \zeta_2(\varpi, \omega, \psi(\omega)) \, d\omega \Big] d\varpi \\
&+ BW^{-1} \Big[\frac{1}{\Gamma(\aleph)} \int_{\varphi_1}^{\varphi_2} (\varphi_2 - \varpi)^{\aleph-1} \Big[\Upsilon(\varpi)\psi(\varpi) + \xi_2(\varpi, \psi(\varpi)) \\
&\quad + \int_{\varphi_0}^{\varpi} \zeta_1(\varpi, \omega, \psi(\omega)) \, d\omega + \int_{\varphi_0}^{b} \zeta_2(\varpi, \omega, \psi(\omega)) \, d\omega \Big] d\varpi \\
&\quad - \int_{\varphi_0}^{\varphi_1} [(\varphi_1 - \varpi)^{\aleph-1} - (\varphi_2 - \varpi)^{\aleph-1}] \Upsilon(\varpi)\psi(\varpi) d\varpi \\
&\quad - \int_{\varphi_0}^{\varphi_1} [(\varphi_1 - \varpi)^{\aleph-1} - (\varphi_2 - \varpi)^{\aleph-1}] \xi_2(\varpi, \psi(\varpi)) d\varpi
\end{aligned}
$$

$$- \int_{\varphi_0}^{\varphi_1} \Big[(\varphi_1 - \varpi)^{\aleph-1} \int_{\varphi_0}^{\varpi} \zeta_1(\varpi, \omega, \psi(\omega))\, d\omega - (\varphi_2 - \varpi)^{\aleph-1} \int_{\varphi_0}^{\varpi} \zeta_1(\varpi, \omega, \psi(\omega))\, d\omega \Big] d\varpi$$
$$- \int_{\varphi_0}^{\varphi_1} \Big[(\varphi_1 - \varpi)^{\aleph-1} \int_{\varphi_0}^{b} \zeta_2(\varphi, \omega, \psi(\omega))\, d\omega - (\varphi_2 - \varpi)^{\aleph-1} \int_{\varphi_0}^{b} \zeta_2(\varphi, \omega, \psi(\omega))\, d\omega \Big] d\varpi \Big\Big\|.$$

Taking the limit as $\varphi_2 \to \varphi_1$, the integral over $[\varphi_1, \varphi_2]$ tends to zero since

$$\int_{\varphi_1}^{\varphi_2} (\varphi_2 - \varpi)^{\aleph-1}\, d\varpi = \frac{(\varphi_2 - \varphi_1)^{\aleph}}{\aleph} \longrightarrow 0, \qquad 0 < \aleph \leq 1.$$

Moreover, since $\frac{1}{2} < \aleph \leq 1$, the control kernel is square-integrable and, by the Cauchy–Schwarz inequality,

$$\frac{1}{\Gamma(\aleph)} \left\| \int_{\varphi_1}^{\varphi_2} (\varphi_2 - \varpi)^{\aleph-1} B\mu(\varpi)\, d\varpi \right\| \leq \frac{M_1}{\Gamma(\aleph)\sqrt{2\aleph - 1}} (\varphi_2 - \varphi_1)^{\aleph - \frac{1}{2}} \|\mu\|_{L^2(\mathcal{J},U)} \longrightarrow 0$$

as $\varphi_2 \to \varphi_1$. The remaining fractional-kernel differences over $[\varphi_0, \varphi_1]$ tend to zero by the dominated convergence theorem. Moreover, the estimates are independent of the particular $\psi \in \Lambda_{\gamma_1}$ because $\|\psi\|_\infty \leq \gamma_1$ and the constants appearing in $(B1)$–$(B7)$ are uniform on Λ_{γ_1}. Therefore,

$$\sup_{\psi \in \Lambda_{\gamma_1}} \|(\Psi\psi)(\varphi_2) - (\Psi\psi)(\varphi_1)\| \longrightarrow 0 \qquad \text{as } \varphi_2 \to \varphi_1,$$

for $\varphi_1, \varphi_2 \in (\varphi_k, \varphi_{k+1}]$. Hence, $\Psi(\Lambda_{\gamma_1})$ is equicontinuous on every impulse-free interval. At each impulsive point φ_k, the corresponding left and right limits are considered separately according to the definition of $PC(\mathcal{J}; \mathcal{X})$. Combining Steps 1–3 with Theorem 2.1, we conclude that $\Psi(\Lambda_{\gamma_1})$ is relatively compact. Hence, Ψ is continuous and compact on Λ_{γ_1}. By Theorem 2.2, Ψ has a fixed point, which provides a solution of (4.1)–(4.2). Consequently, the system is controllable over $\mathcal{J} = [\varphi_0, b]$. This completes the proof of the theorem. □

5. Example and numerical verification

We consider a numerical example of the Caputo fractional impulsive Volterra–Fredholm integro-differential equation introduced in (4.1)–(4.2). In accordance with the assumption imposed in Theorem (4.1), the fractional order is selected as $\frac{1}{2} < \aleph \leq 1, \aleph = 0.75$. The computational interval is taken as $\mathcal{J} = [\varphi_0, b] = [0, 0.5]$, with initial and prescribed terminal states $\psi(0) = \psi_0 = 0.1, \psi(0.5) = \psi_1 = 0.2$.

For the numerical illustration, the nonlinear and integral terms are explicitly specified by

$$\Upsilon(\varphi) = 0.1, \qquad \xi_1(\varphi, \psi) = 0.2\psi + 0.3\varphi, \qquad \xi_2(\varphi, \psi) = 0.2\psi + 0.3,$$

$$\zeta_1(\varphi, \varpi, \psi) = 0.4\psi + 0.3, \qquad \zeta_2(\varphi, \varpi, \psi) = 0.3\psi + 0.3,$$

and the control operator is chosen as $(Bu)(\varphi) = 0.2u(\varphi)$. A single impulse is considered at $\varphi_1 = 0.25$, with $I_1(\psi) = 0.2\psi$.

Thus, the impulsive condition is $\psi(0.25^+) - \psi(0.25^-) = 0.2\psi(0.25^-)$. Consequently, the numerical problem corresponding to (4.1)–(4.2) is

$$\begin{aligned} {}^{C}D^{0.75}\left[\psi(\varphi) - 0.2\psi(\varphi) - 0.3\varphi\right] &= 0.1\psi(\varphi) + 0.2\psi(\varphi) + 0.3 \\ &\quad + \int_0^{\varphi} \left[0.4\psi(\varpi) + 0.3\right] d\varpi \\ &\quad + \int_0^{0.5} \left[0.3\psi(\varpi) + 0.3\right] d\varpi + 0.2u(\varphi), \end{aligned} \tag{5.1}$$

subject to

$$\psi(0) = 0.1, \qquad \psi(0.25^+) - \psi(0.25^-) = 0.2\psi(0.25^-), \qquad \psi(0.5) = 0.2. \tag{5.2}$$

For the theoretical parameter verification, we use

$$b = 0.5, \quad \aleph = 0.75, \quad \gamma_1 = 0.3, \quad M_1 = 0.2, \quad M_2 = 0.4,$$

$$\|\psi_0\| = 0.1, \qquad \|\psi_1\| = 0.2, \qquad \|\Upsilon\|_\infty = 0.1,$$

$$L_{\xi_1} = 0.2, \quad L^*_{\xi_1} = 0.3, \quad L_{\xi_2} = 0.2, \quad L^*_{\xi_2} = 0.3,$$

$$L_{\zeta_1} = 0.4, \quad L^*_{\zeta_1} = 0.3, \quad L_{\zeta_2} = 0.3, \quad L^*_{\zeta_2} = 0.3,$$

and

$$m = 1, \text{ and } \lambda^*_2 = 0.2.$$

With these values, the constant appearing in Theorem 4.1 is evaluated as

$$\begin{aligned} \mathfrak{Q}_1 &= \frac{b^{\aleph}}{\Gamma(\aleph+1)} M_1 M_2 \|\psi_1\| \\ &\quad + \left(1 + \frac{b^{\aleph}}{\Gamma(\aleph+1)} M_1 M_2\right)\left[\|\psi_0\| + \frac{\|\Upsilon\|_\infty b^{\aleph}\gamma_1}{\Gamma(\aleph+1)} + \frac{b^{\aleph}}{\Gamma(\aleph+1)}\left(L_{\xi_2}\gamma_1 + L^*_{\xi_2}\right)\right. \\ &\quad \left. + \frac{b^{\aleph+1}}{(\aleph+1)\Gamma(\aleph)}\left(L_{\zeta_1}\gamma_1 + L^*_{\zeta_1}\right) + \frac{b^{\aleph+1}}{(\aleph+1)\Gamma(\aleph)}\left(L_{\zeta_2}\gamma_1 + L^*_{\zeta_2}\right)\right] \\ &\quad + \left(\|\xi_1(0,\psi_0)\| + L_{\xi_1} + L^*_{\xi_1}\gamma_1\right)(1 + M_1 M_2) + M_1 M_2 m\lambda^*_2. \end{aligned}$$

Since

$$\|\xi_1(0,\psi_0)\| = 0.2(0.1) = 0.02,$$

the above expression gives

$$\mathfrak{Q}_1 \approx 0.84981 < 1.$$

Hence, under the assumptions of Theorem 4.1, the corresponding system satisfies the stated sufficient condition for controllability.

5.1. Numerical procedure

The numerical solution is computed from the mild integral formulation corresponding to (5.1). The interval $[0, 0.5]$ is divided into N uniform subintervals:

$$\varphi_n = nh, \qquad h = \frac{0.5}{N}, \qquad n = 0, 1, \ldots, N.$$

For the principal computation, $N = 200$ and hence $h = 0.0025$. The weakly singular fractional integral is approximated by the product-integration formula

$$\frac{1}{\Gamma(\aleph)} \int_0^{\varphi_n} (\varphi_n - \varpi)^{\aleph-1} F(\varpi)\, d\varpi \approx \frac{h^{\aleph}}{\Gamma(\aleph+1)} \sum_{j=0}^{n-1} \left[(n-j)^{\aleph} - (n-j-1)^{\aleph}\right] F(\varphi_j). \tag{5.3}$$

The Volterra and Fredholm integral terms are evaluated by numerical quadrature. The resulting nonlinear discrete mild equation is solved by fixed-point iteration with relaxation. The iteration is terminated when the maximum change between two successive iterates is less than 10^{-11}.

The constant control value is determined numerically so that the terminal condition $\psi(0.5) = \psi_1 = 0.2$ is satisfied. The numerical implementation was performed in Python using NumPy, SciPy, and Matplotlib.

To quantify the accuracy of the computation, the maximum residual of the discretized mild equation is defined by

$$E_{\text{mild}} = \max_{0 \le n \le N} |R_n|, \tag{5.4}$$

where R_n denotes the difference between the computed numerical solution and the corresponding right-hand side of the discrete mild formulation. The terminal-state error is measured by

$$E_{\text{terminal}} = |\psi(b) - \psi_1|. \tag{5.5}$$

The impulsive contribution is evaluated directly from

$$\Delta\psi(\varphi_1) = I_1(\psi(\varphi_1^-)) = 0.2\psi(\varphi_1^-). \tag{5.6}$$

5.2. Numerical results

For $N = 200$, the computed control is

$$u = -3.7147110159.$$

The numerical solution gives

$$\psi(0.25^-) = 0.0970443393,$$

and therefore, from the prescribed impulsive condition,

$$\Delta\psi(0.25) = 0.2\psi(0.25^-) = 0.0194088679.$$

Consequently,

$$\psi(0.25^+) = 0.1164532072.$$

At the terminal point,

$$\psi(0.5) = 0.2000000000,$$

which agrees with the prescribed terminal state $\psi_1 = 0.2$.

The maximum mild-equation residual is

$$E_{\text{mild}} = 4.2857939420 \times 10^{-12},$$

while the terminal-state error is

$$E_{\text{terminal}} = 5.5577764613 \times 10^{-12}.$$

These small values indicate that the computed discrete solution satisfies the implemented mild formulation and the prescribed terminal condition to numerical tolerance.

The principal numerical results are summarized in Table 1.

Table 1. Numerical results for the Caputo fractional impulsive VFIDE.

Quantity	Numerical value
Fractional order $\aleph$	0.75
Number of grid intervals N	200
Step size h	0.0025
Impulse point φ_1	0.25
Computed control u	−3.7147110159
$\psi(\varphi_1^-)$	0.0970443393
$\Delta\psi(\varphi_1)$	0.0194088679
$\psi(\varphi_1^+)$	0.1164532072
$\psi(0.5)$	0.2000000000
E_{mild}	$4.2857939420 \times 10^{-12}$
E_{terminal}	$5.5577764613 \times 10^{-12}$

5.3. Grid-refinement study

To examine the numerical stability with respect to the computational grid, calculations were repeated for $N = 100$, $N = 200$, and $N = 400$. The corresponding results are presented in Table 2. The computed control values remain close as the grid is refined, while both the mild-equation residual and terminal-state error remain at the order of 10^{-12}. Thus, the numerical computation exhibits stable behavior over the tested grids.

Table 2. Grid-refinement results.

N	h	u	E_{mild}	E_{terminal}
100	0.00500	−3.712047	4.198947×10^{-12}	5.437650×10^{-12}
200	0.00250	−3.714711	4.285794×10^{-12}	5.557776×10^{-12}
400	0.00125	−3.716041	4.338002×10^{-12}	5.628747×10^{-12}

The small variation in the computed control values under grid refinement confirms the numerical stability of the reported controlled trajectory. The residual values remain at the numerical iteration-tolerance level and are therefore used as a consistency check of the discrete mild formulation rather than as an estimate of the discretization order. The numerical experiment complements the theoretical controllability result established in Theorem 4.1.

6. Graphical representation of the Caputo fractional impulsive VFIDE

This section presents graphical representations of the numerical solution obtained from the test problem (5.1)–(5.2). The figures illustrate the continuous evolution between the impulse point, the prescribed impulsive jump at $\varphi_1 = 0.25$, and the attainment of the prescribed terminal state $\psi_1 = 0.2$. The graphical results are intended to complement the quantitative numerical verification presented in Section 5; the theoretical controllability conclusion follows from Theorem 4.1.

6.1. Numerical solution trajectory

Figure 1 presents the computed trajectory of $\psi(\varphi)$ on the interval $[0, 0.5]$. The trajectory starts from

$$\psi(0) = 0.1$$

and evolves continuously up to the impulse point $\varphi_1 = 0.25$. At this point, the solution undergoes the prescribed impulsive change

$$\Delta\psi(0.25) = 0.2\psi(0.25^-) = 0.0194088679.$$

The evolution after the impulse is then continued until the terminal point $\varphi = 0.5$.

The numerical solution is therefore piecewise continuous, with the discontinuity occurring at the prescribed impulse point. The computed terminal value is

$$\psi(0.5) = 0.2000000000,$$

which agrees with the prescribed terminal state.

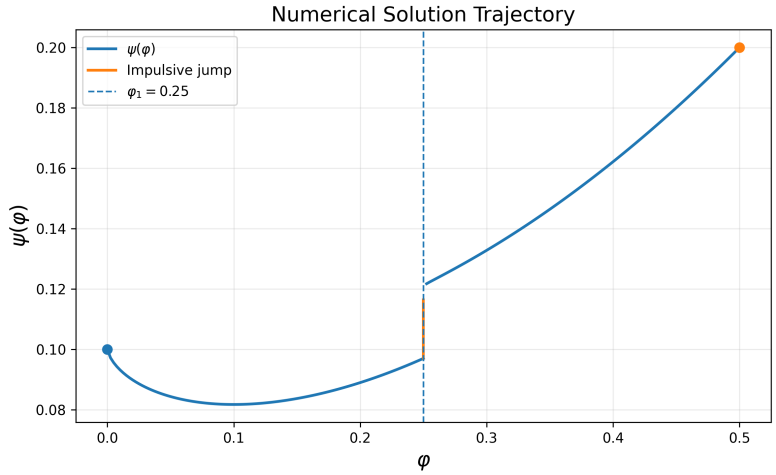


Figure 1. Numerical solution trajectory $\psi(\varphi)$ with the impulsive jump at $\varphi_1 = 0.25$.

6.2. *Impulsive contribution*

Figure 2 displays the magnitude of the impulsive contribution at $\varphi_1 = 0.25$. Since

$$I_1(\psi) = 0.2\psi,$$

the computed value

$$\psi(0.25^-) = 0.0970443393$$

produces the impulsive contribution

$$\Delta\psi(0.25) = I_1(\psi(0.25^-)) = 0.0194088679.$$

Thus, the figure provides a direct visualization of the magnitude of the prescribed impulse used in the numerical example.

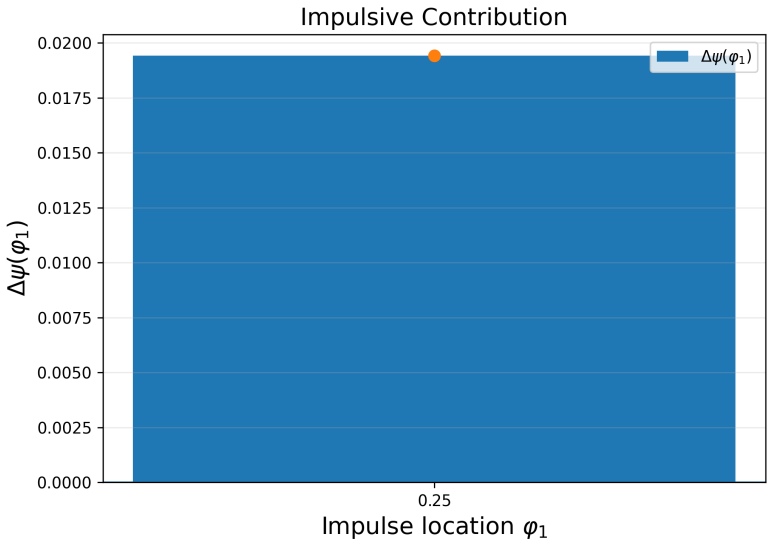


Figure 2. Computed impulsive contribution $\Delta\psi(\varphi_1)$ at the impulse point $\varphi_1 = 0.25$.

6.3. *Terminal-state verification*

Figure 3 compares the computed trajectory with the prescribed terminal state $\psi_1 = 0.2$. The dashed horizontal line represents the target value, while the terminal marker identifies the computed value

$$\psi(0.5) = 0.2000000000.$$

The corresponding terminal-state error is

$$E_{\text{terminal}} = |\psi(0.5) - 0.2| = 5.557776 \times 10^{-12}.$$

Therefore, the computed controlled trajectory reaches the prescribed terminal state to numerical tolerance. It is emphasized that this figure is a numerical verification of the selected controlled trajectory and should not be interpreted independently as a proof of controllability. The controllability of the system follows from the sufficient conditions established in Theorem 4.1.

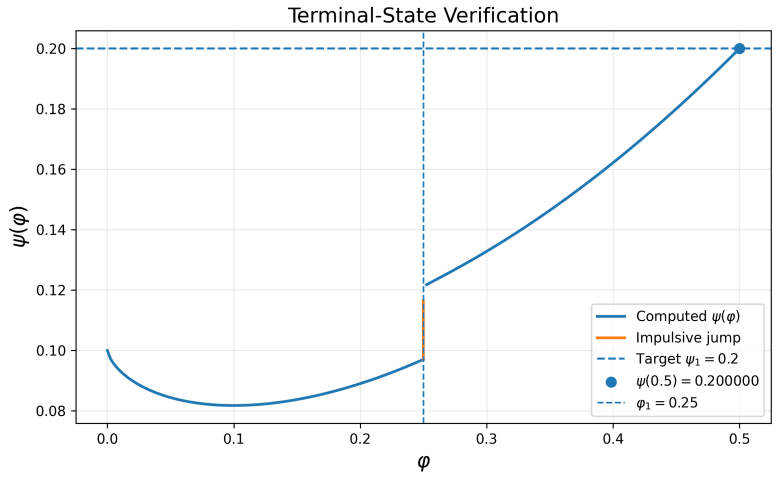


Figure 3. Terminal-state verification for the computed controlled trajectory.

6.4. Numerical interpretation

The numerical results provide a consistent illustration of the behavior of the Caputo fractional impulsive VFIDE. The trajectory evolves continuously between the initial point and the impulse point, undergoes the prescribed jump at $\varphi_1 = 0.25$, and subsequently evolves toward the target terminal state. The computed control

$$u = -3.7147110159$$

produces the terminal value $\psi(0.5) = 0.2$.

The maximum residual of the discretized mild equation is of order 10^{-12}, and the terminal-state error is also of order 10^{-12}. Furthermore, the grid-refinement results for $N = 100$, 200, and 400 exhibit stable numerical behavior. These observations support the numerical consistency of the implemented test problem and complement the theoretical controllability result established in Theorem 4.1.

7. Application to Solana cryptocurrency price modeling using the proposed fractional impulsive VFIDE framework

In this section, we illustrate the application of the fractional impulsive Volterra–Fredholm integro-differential model to a real financial dataset to demonstrate its relevance to a practical modeling problem. The price time series of Solana (SOL) exhibits substantial temporal variation and abrupt price movements, together with possible temporal dependence and nonlocal interactions, making it a suitable real-data setting for illustrating the proposed fractional impulsive VFIDE framework. These characteristics are consistent with the mathematical structure of the fractional Caputo impulsive VFIDE investigated in the previous sections of this work.

7.1. Data description and preprocessing

The dataset consists of the daily closing prices of Solana (SOL) obtained from Investing.com [30] for the period from January 1, 2025–December 1, 2025. The dataset contains 335 daily observations. The numerical modeling time index was then uniformly spaced and the dates were converted to the

numerical variable

$$\varphi \in [\varphi_0, b] = [0, 334],$$

where $\psi(\varphi)$ denotes the observed Solana closing price at time φ. The analysis was preceded by data cleaning, where any missing values, if present, were corrected, dates were standardized, and all numerical attributes were converted to floating-point format. The initial and final observed closing prices were 194.157 USD and 126.730 USD, respectively. The processed dataset used in the numerical experiments is provided as supplementary material, subject to the terms and conditions of the original data provider.

Figure 4 presents the daily closing-price trajectory of Solana. The observed series exhibits substantial temporal variation and abrupt price movements, providing a suitable real-data setting for illustrating the fractional and impulsive components of the proposed model.

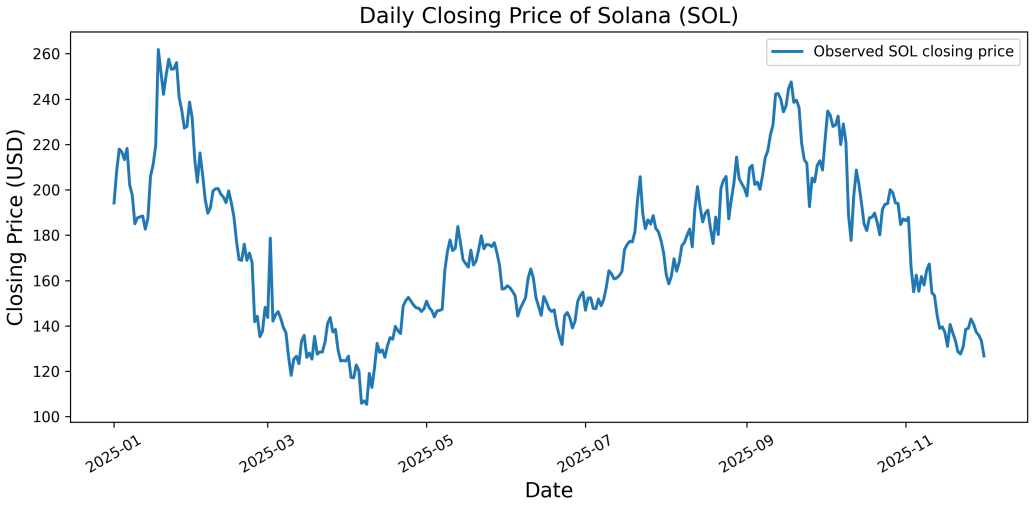


Figure 4. Daily closing price of Solana (SOL) from January 1 to December 1, 2025.

The observed trajectory contains periods of relatively gradual variation together with abrupt changes in the closing price. Such features motivate the use of a modeling framework capable of incorporating memory effects, nonlocal interactions, and impulsive changes. The present application is therefore used to illustrate how these characteristics can be represented within the proposed fractional impulsive VFIDE framework.

7.2. Identification of impulsive price movements

The data modeling was performed using the uncontrolled fractional impulsive VFIDE described by Eq (3.1), coupled with the impulsive condition $\Delta\psi(\varphi_k) = I_k(\psi(\varphi_k^-))$ at the detected shock points φ_k. The major impulsive points were identified according to the magnitude of the day-to-day price change using the criterion

$$|\psi(\varphi + 1) - \psi(\varphi)| > \tau,$$

where τ is a threshold determined from the observed price-change series and is expressed as a prescribed multiple of the median absolute deviation. In the present experiment, the threshold multiplier was selected as $\kappa = 3.0$. Letting $\Delta\psi(\varphi) = \psi(\varphi + 1) - \psi(\varphi)$ and MAD denote the median

absolute deviation of the price-change series, the threshold was defined as

$$\tau = \kappa\,\mathrm{MAD}(\Delta\psi).$$

For the present dataset, the median absolute deviation was MAD = 4.299, giving the threshold $\tau = 12.897$. Accordingly, 25 impulsive observations were identified using the prescribed criterion. Impulsive points are shown in Figure 5, where the red markers represent the observations detected by the prescribed impulsive-point criterion.

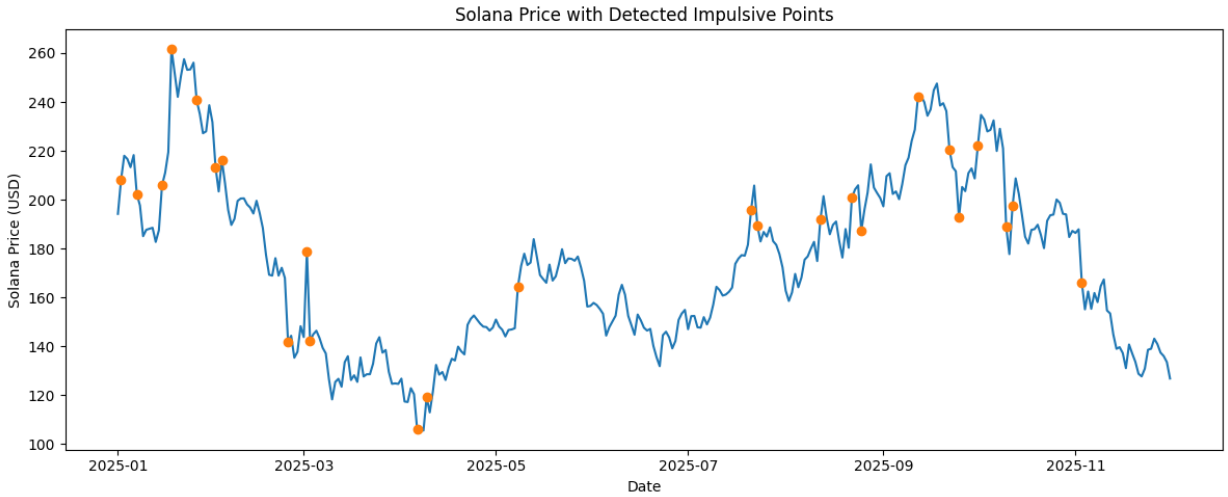


Figure 5. Solana closing-price trajectory with the detected impulsive points marked in red according to the prescribed price-change threshold.

7.3. Fractional impulsive VFIDE model fitting

The order of the fractional $\aleph$ was estimated using a procedure that minimizes the mean square error between the observations and the numerical solution of (3.1). The estimated optimal fractional order was $\aleph = 0.852424$, which satisfies the theoretical restriction $\frac{1}{2} < \aleph \leq 1$ imposed in the controllability analysis. The estimated fractional order provides a model-based representation of the memory characteristics present in the observed price series.

The parameters associated with Υ, ξ_1, ξ_2, ζ_1, and ζ_2 were calibrated using a nonlinear least-squares fitting procedure within the proposed fractional impulsive VFIDE framework. The same numerical discretization framework described in Section 5 was used for the numerical evaluation of the fractional and integral terms. The resulting fitted trajectory is compared with the observed Solana closing-price series in Figure 6. The purpose of this fitting procedure is to illustrate the ability of the proposed mathematical structure to represent the temporal behavior and abrupt changes present in the considered financial data.

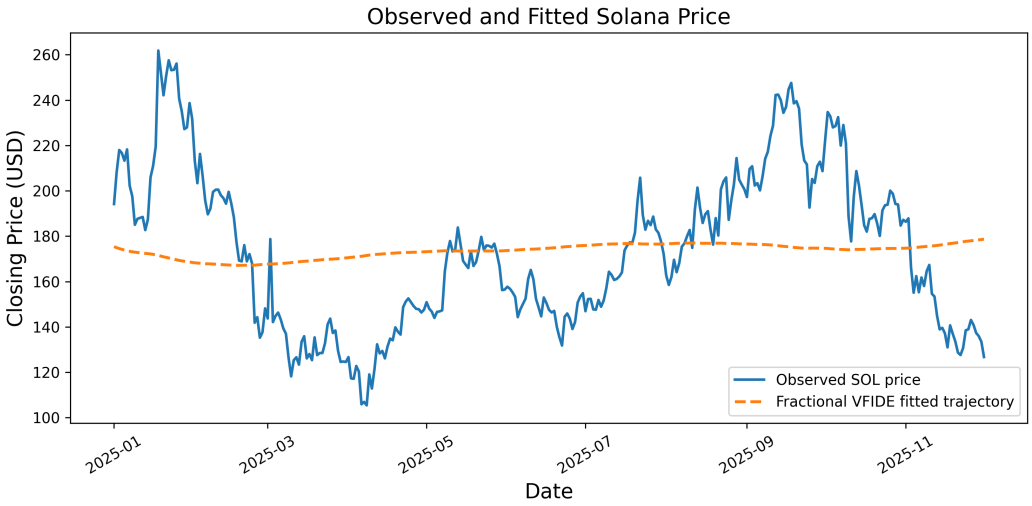


Figure 6. Comparison between the observed Solana closing price and the trajectory fitted using the proposed fractional impulsive VFIDE model.

The fitted trajectory is presented as a qualitative representation of the observed price dynamics rather than as an independently validated forecasting model. In particular, the present application is intended to demonstrate the implementation of the proposed fractional impulsive VFIDE framework on real financial data.

7.4. Controlled scenario analysis using the VFIDE framework

The control term $(Bu)(\varphi)$ of the fractional impulsive VFIDE model, outlined in Eq (4.1), is incorporated to investigate the response of the modeled trajectory to a prescribed control input. Based on the controllability result established in Theorem 4.2, the control mechanism provides a mathematical framework for steering the model state toward a prescribed reference trajectory $\psi_d(\varphi)$. In the present application, this control formulation is used as a scenario-analysis tool to examine the effect of controlled trajectory regulation on the modeled Solana price dynamics.

In Figure 7, we present the historical data, the model-fitted trajectory, and the controlled trajectory extending beyond the historical observation period. The figure illustrates the different stages of the analysis, beginning with the observed data, followed by the model approximation, and finally the controlled trajectory generated using the controlled VFIDE framework.

The controlled model was applied after the historical observation period to examine the response of the modeled trajectory to the prescribed control input. The 2025 observations provide the historical information used in the fractional-memory component, while the subsequent trajectory represents a controlled model scenario rather than an independently validated market forecast. The resulting trajectory illustrates how the control mechanism can modify the evolution of the modeled state and steer it toward the prescribed reference region. This experiment demonstrates the potential use of the controllability framework for trajectory regulation and scenario analysis in financial dynamical systems.

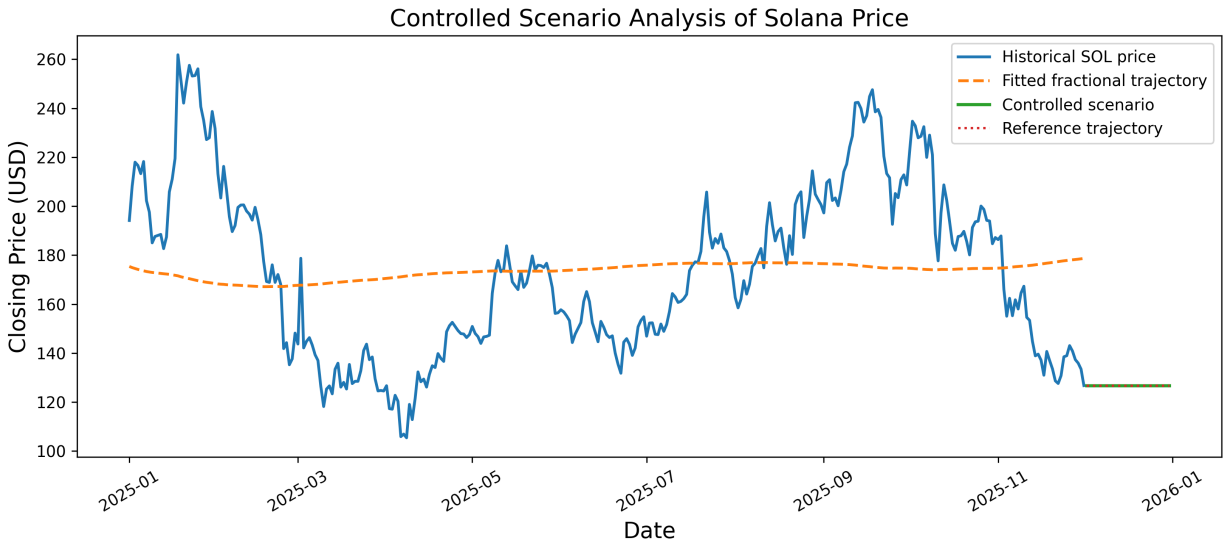


Figure 7. Controlled scenario analysis of the Solana price using the fractional impulsive VFIDE framework. The controlled trajectory is compared with the historical and fitted trajectories and a prescribed reference trajectory.

7.5. Discussion

The proposed fractional impulsive Volterra–Fredholm integro-differential framework is a unified mathematical structure that allows the representation of dynamical systems with memory effects, nonlocal interactions, and abrupt state changes. The use of these mathematical characteristics in the context of Solana (SOL) cryptocurrency illustrates the potential for these characteristics to be applied to the modeling of the dynamics of cryptocurrency prices. A way to account for memory effects is to let the fractional derivative be dependent on the past evolution of the state, as done in the Caputo fractional derivative. Furthermore, the Volterra and Fredholm terms of the integral are finite time and global time contributions, respectively. The impulsive part also enables the explicit inclusion of abrupt changes in the modeled state, thus going beyond the continuous description of the dynamics.

The controllability part of the extended model is capable of studying the influence of an admissible control input on the trajectory of the system. The key application of the controlled formulation is as a scenario analysis tool to understand how the modeled trajectory can be altered to proceed through a desired reference range. The numerical results support the theoretical developments by providing examples of real financial data on which the framework is applied. The historical-price trajectory is the actual trajectory, the fitted trajectory shows how the actual dynamics are represented in the proposed model, and the impulsive representation looks for abrupt changes following the specified detection rule. The controlled scenario also illustrates how the controllability formulation can be used for trajectory-regulation analysis.

The overall results of the Solana application show how the proposed fractional impulsive VFIDE model can be applied to a real-data modeling problem with temporal dependence, nonlocal effects, and abrupt variations. The controlled trajectory is an example of trajectory regulation in the proposed mathematical framework. The present study, however, is designed to be primarily a mathematical-modeling and scenario-analysis application and not a fully validated cryptocurrency forecasting

system. The predictive capability and the generalization of the proposed model should be evaluated in further investigations including out-of-sample validation, further observation periods, different impulse-detection criteria, and comparisons with other statistical and machine-learning methods.

8. Conclusions

In this work, an impulsive neutral Volterra–Fredholm integro-differential equation with a Caputo fractional derivative was studied and a mathematical framework was provided for the study of existence and controllability. The existence of solutions was proved with the help of the Schauder fixed point theorem, based on appropriate assumptions for the fractional order, nonlinear functions, integral operators, and system components. Furthermore, an admissible control was developed to enable the system state to be controlled toward a given target state and a controllability result was obtained for the corresponding system. The theoretical results give mathematical tools for the study of dynamical systems with fractional memory, nonlocal integral interactions, and impulsive effects in a unified formulation.

Then the theoretical framework was illustrated by a numerical example, where all the system functions, operators, initial and final conditions, impulse conditions, discretization procedure, and numerical parameters were explicitly given. A product-integration approximation was used for the fractional integral representation, numerical quadrature for Volterra and Fredholm terms, and a fixed-point iteration procedure was also utilized. The numerical results confirmed the prescribed impulsive condition and the terminal constraint within the numerical tolerance adopted, and the grid refinement calculations showed stable numerical behavior. The calculations gave a numerical example of the theory presented in the previous sections, which is repeatable.

The suggested framework was also used to model closing-price data of a cryptocurrency, Solana (SOL), during the time frame of January 1, 2025–December 1, 2025. The fractional part was used to account for memory effects, the Volterra and Fredholm parts were added to capture the nonlocal contributions, and the impulsive part was added to capture abrupt variations identified from the observed price-change series. The controlled formulation was then used for scenario analysis to investigate the effect of a permissible control input on the simulated trajectory. The outcome numerical representations illustrate how fractional and nonlocal, impulsive and controllability properties can be represented in the unified framework of mathematics in the modeling of real data. The Solana study is not designed to be a complete or accurate model for predicting cryptocurrency prices, but rather an illustrative and simulated example.

There are multiple avenues left to explore in the future. The proposed framework can be generalized to the variable-order, distributed-order, and/or fractional operators, to systems with state-dependent delays, as well as to systems with stochastic perturbations and more general impulsive mechanisms. Applications to other systems such as financial, engineering, biological, and signal-processing systems with memory and impulsive behavior could also be considered. Future financial applications could benefit from the implementation of longer time horizons, out-of-sample validation, different impulse-detection methods, and systematic comparisons with existing methods in statistical or machine-learning methods. These extensions would further investigate the applicability, robustness, and predictability of fractional impulsive Volterra–Fredholm models for complex dynamical systems.

Author contributions

P.R, Y.P, S.S.S, and M.J.H wrote and edited the main manuscript text, created the software and coding, and prepared the results. All authors have read and approved the final version of the manuscript for publication.

Use of Generative-AI tools declaration

The authors declare they have not used Artificial Intelligence (AI) tools in the creation of this article.

Acknowledgments

The work of Mohammadjavad Habibivostakolaei was funded by the High-Level Talent Research Start-Up Project funding of Henan Academy of Sciences (project no. 241819245).

The authors thank the editor and referees for their valuable suggestions and comments.

Conflict of interest

The authors declare that they have no conflict of interest.

Data availability statement

The Solana (SOL) historical price data used in this study were obtained from Investing.com [30]. The processed dataset used for the numerical experiments is provided as supplementary material to this article.

References

1. A. A. Kilbas, H. M. Srivastava, J. J. Trujillo, *Theory and applications of fractional differential equations*, Amsterdam: Elsevier, **204** (2006).
2. Y. Zhou, J. Wang, L. Zhang, Basic theory of fractional differential equations, Singapore: World Scientific, 2016. https://doi.org/10.1142/10238
3. B. Ahmad, S. Sivasundaram, Some existence results for fractional integro-differential equations with nonlinear conditions, *Commun. Appl. Anal.,* **12** (2008), 107. Available from: `https://api.semanticscholar.org/CorpusID:59433185`.
4. S. Harikrishnan, D. Vivek, E. M. Elsayed, Existence and stability of integro differential equation with generalized proportional fractional derivative, *J. Contemp. Math. Anal.,* **58** (2023), 253–263. https://doi.org/10.3103/S1068362323040040
5. K. Hattaf, A new generalized definition of fractional derivative with non-singular kernel, *Computation,* **8** (2020), 49. https://doi.org/10.3390/computation8020049
6. A. Hamoud, K. Ghadle, Some new uniqueness results of solutions for fractional Volterra-Fredholm integro-differential equations, *Iranian J. Math. Sci. Inform.,* **17** (2022), 135–144. Available from: `http://ijmsi.ir/article-1-1366-en.html`.

7. A. Hamoud, N. Mohammed, K. Ghadle, Existence and uniqueness results for Volterra-Fredholm integro differential equations, *Adv. Theory Nonlinear Anal. Appl.,* **4** (2020), 361–372. Available from: https://atnaea.org/index.php/journal/article/view/148.
8. A. Ndiaye, F. Mansal, Existence and uniqueness results of Volterra-Fredholm integro-differential equations via Caputo fractional derivative, *J. Math.,* **2021** (2021), 1–8. https://doi.org/10.1155/2021/5623388
9. A. Toma, O. Postavaru, A numerical method to solve fractional Fredholm-Volterra integro-differential equations, *Alexandria Eng. J.,* **68** (2023), 469–478. https://doi.org/10.1016/j.aej.2023.01.033
10. H. HamaRashid, H. M. Srivastava, M. Hama, P. O. Mohammed, M. Y. Almusawa, D. Baleanu, Novel algorithms to approximate the solution of nonlinear integro-differential equations of Volterra-Fredholm integro type, *AIMS Math.,* **8** (2023), 14572–14591. https://doi.org/10.3934/math.2023745
11. W. Jiang, Z. Chen, Solving a system of linear Volterra integral equations using the new reproducing kernel method, *Appl. Math. Comput.,* **219** (2013), 10225–10230. https://doi.org/10.1016/j.amc.2013.03.123
12. S. Hussain, M. Sarwar, N. Mlaiki, F. Azmi, Existence and controllability of fractional semilinear mixed Volterra-Fredholm integro differential equation, *Alex. Eng. J.,* **73** (2023), 259–267. https://doi.org/10.1016/j.aej.2023.04.029
13. E. Hernandez, D. O'Regan, Controllability of Volterra Fredholm type systems in Banach spaces, *J. Franklin I.,* **346** (2009), 95–101. https://doi.org/10.1016/j.jfranklin.2008.08.001
14. C. Dineshkumar, V. Vijayakumar, R. Udhayakumar, A. Shukla, K. S. Nisar, Controllability discussion for fractional stochastic Volterra Fredholm integro-differential systems of order $1 < r < 2$, *Int. J. Nonlinear Sci. Numer. Simul.,* **24** (2023), 33. https://doi.org/10.1515/ijnsns-2021-0479
15. V. Jurdjevic, J. P. Quinn, Controllability and stability, *J. Differ. Equations,* **28** (1978), 381–389. http://dx.doi.org/10.1016/0022-0396(78)90135-3
16. S. Hussain, M. Sarwar, G. Rahmat, H. Aydi, M. De La Sen, Mild solutions and controllability of fractional evolution inclusions of Clarke's subdifferential type with nonlocal conditions in Hilbert spaces, *Alex. Eng. J.,* **80** (2023), 58–73. https://doi.org/10.1016/j.aej.2023.08.008
17. S. Hussain, M. Sarwar, K. S. Nisar, K. Shah, Controllability of fractional differential evolution equation of order $\gamma \in (1, 2)$ with nonlocal conditions, *AIMS Math.,* **8** (2023), 14188–14206. https://doi.org/10.3934/math.2023726
18. G. R. Gautam, S. Pinelas, M. Kumar, N. Arya, J. Bishnoi, On the solution of $\mathcal{T}$-controllable abstract fractional differential equations with impulsive effects, *CUBO Math. J.,* **8** (2023), 363–386. http://dx.doi.org/10.56754/0719-0646.2503.363
19. G. R. Gautam, M. Kumar, A. Dwivedi, G. Rani, N. Arya, J. Bishnoi, Some sufficient conditions of existence and trajectory controllability for impulsive and initial value fractional order functional differential equations, *Results Control Optim.,* **12** (2023), 100237. https://doi.org/10.1016/j.rico.2023.100237

20. M. M. Raja, A. Shukla, J. J. Nieto, V. Vijayakumar, K. S. Nisar, A note on the existence and controllability results for fractional integrodifferential inclusions of order $r \in (1, 2]$ with impulses, *Qual. Theory Dyn. Syst.,* **21** (2022), 150. https://doi.org/10.1007/s12346-022-00681-z
21. Y. K. Ma, M. M. Raja, A. Shukla, V. Vijayakumar, K. S. Nisar, K. Thilagavathi, New results on approximate controllability of fractional delay integrodifferential systems of order $1 < r < 2$ with Sobolev-type, *Alex. Eng. J.,* **81** (2023), 501–518. https://doi.org/10.1016/j.aej.2023.09.043
22. M. Johnson, M. M. Raja, V. Vijayakumar, A. Shukla, Optimal control results for fractional differential hemivariational inequalities of order $r \in (1, 2)$, *Optimization,* **74** (2025), 1–25. https://doi.org/10.1080/02331934.2024.2306304
23. L. Sadek, Control theory for fractional differential Sylvester matrix equations with Caputo fractional derivative, *J. Vib. Control,* **31** (2025), 1586–1602. https://doi.org/10.1177/10775463241246430
24. K. Ramalakshmi, M. E. Samei, Mathematical model of optimal control for endometrial cancer with treatments dostarlimab and chemotherapy using Caputo derivative, *Sci. Rep.,* **15** (2025), 39490. https://doi.org/10.1038/s41598-025-23149-x
25. E. Aljarallah, K. Venkatachalam, E. S. El-Hady, Caputo-Fabrizio fractional integro-differential equations: Existence, uniqueness, and β-Ulam stability results for the solutions in a Banach space, *AIMS Math.,* **11** (2026), 1527–1546. https://doi.org/10.3934/math.2026064
26. M. Sher, K. Shah, Z. Ali, T. Abdeljawad, M. A. Alqudah, Using deep neural network in computational analysis of coupled systems of fractional integro-differential equations, *J. Comput. Appl. Math.,* **474** (2026), 116912. https://doi.org/10.1016/j.cam.2025.116912
27. V. Antipov, Y. Kabanov, On the integro-differential equation arising in the ruin problem for non-life insurance models with investment, *Mathematics,* **14** (2026), 1035. https://doi.org/10.3390/math14061035
28. P. Raghavendran, Y. Parthiban, A hybrid neural network approach to controllability in Caputo fractional neutral integro-differential systems for cryptocurrency forecasting, *Fractal Fract.,* **10** (2026), 268. https://doi.org/10.3390/fractalfract10040268
29. D. R. Smart, *Fixed point theorems*, Vol. 66, Cambridge: Cambridge University Press, 1980. ISBN: 0521298334, 9780521298339.
30. *Solana historical data*, Investing.com, 2025. Available from: `https://www.investing.com/crypto/solana/historical-data`.



© 2026 the Author(s), licensee AIMS Press. This is an open access article distributed under the terms of the Creative Commons Attribution License (http://creativecommons.org/licenses/by/4.0)